Differences in size and number of embryonic type-II neuroblast lineages correlate with divergent timing of central complex development between beetle and fly

Authors: Simon Rethemeier[1,2], Sonja Fritzsche[1], Dominik Mühlen[1], Gregor Bucher[1] and Vera S. Hunnekuhl[1]*

* Author for correspondence

[1] University of Göttingen, Johann-Friedrich-Blumenbach Institute, GZMB, Department of Evolutionary Developmental Genetics, Germany

[2] University Medical Center Göttingen (UMG), Germany

Abstract

Despite its conserved basic structure, the morphology of the insect brain and the timing of its development underwent evolutionary adaptations. However, little is known about the developmental processes that create this diversity. The central complex is a brain centre required for multimodal information processing and an excellent model to understand neural development and divergence. It is produced in large parts by type-II neuroblasts, which produce intermediate progenitors, another type of cycling precursor, to increase their neural progeny. These neural stem cells are believed to be conserved among insects, but little is known on their molecular characteristics in insects other than flies. *Tribolium castaneum* has emerged as a valuable new insect model for brain development and evolution. However, type-II neuroblast lineages and their role in central complex development have so far not been studied in this beetle.

Using CRISPR-Cas9 we created a fluorescent enhancer trap marking expression of *Tribolium fez/earmuff*, a key marker for type-II neuroblast derived intermediate progenitors. Using combinatorial labelling of further markers including *Tc-pointed*, *Tc-deadpan*, *Tc-asense* and *Tc-prospero* we characterized the type-II neuroblast lineages present in the *Tribolium* embryo and their sub-cell-types. Intriguingly, we found 9 type-II neuroblast lineages per hemisphere in the *Tribolium* embryo while *Drosophila* produces only 8 per brain hemisphere. In addition, these lineages are significantly larger at the embryonic stage of *Tribolium* than they are in *Drosophila* and contain more intermediate progenitors. Finally, we mapped these lineages to the domains of early expressed head patterning genes. Notably, *Tc-otd* is absent from all type-II neuroblasts and intermediate progenitors, whereas

Tc-six3 marks an anterior subset of the type-II-lineages. The placodal marker *Tc-six4* specifically marks the territory where anterior medial type-II neuroblasts differentiate.

In conclusion, we identified a conserved pattern of gene expression in holometabolan central complex forming type-II neuroblast lineages, and conserved head patterning genes emerged as new candidates for conferring spatial identity to individual lineages. The higher number and greater lineage size of the embryonic type-II neuroblasts in the beetle correlate with a previously described embryonic phase of central complex formation which is not found in the fly. These findings stipulate further research on the causal link between timing of stem cell activity and temporal and structural differences in central complex development.

Introduction

Neural development of insects allows to study molecular and cellular principles in easy to manipulate invertebrate models. The fruit fly *Drosophila melanogaster* (*Drosophila* hereafter) has mostly been used for this purpose, making it one of the best understood models for neurogenesis [1,2]. However, it has remained a puzzle how the huge ecological diversity of insects and the divergent neural anatomies that are adapted to different niches [3,4] evolved. Furthermore, *Drosophila* may in many instances not be a good representation of insect development and some processes are derived in the fly lineage [5–7]. For these reasons the beetle *Tribolium castaneum* (*Tribolium* hereafter) has been introduced as an additional model for insect neural development [8–11]. *Tribolium* is a grain storage pest and all stages live in flour, hence there is no major transition of habitat or lifestyle between the larval and adult stage as in flies. However, when compared to *Drosophila* the larvae are more mobile through the use of walking legs which allows them to navigate within or between food sources [3,6,10]. In this beetle many molecular genetic manipulation and labelling methods have been established [12–16]. Specifically, labelling of neural cell types in *Tribolium* has been facilitated by the advent of CRISPR-Cas9 [12,15,17]. Another factor that makes *Tribolium* an informative model for the understanding of insect brain development is the more conserved development of the head neuroectoderm facilitating the identification of specific neurogenic domains and allowing cross-species comparisons [11,18,19].

The insect central complex is an anterior, midline spanning neuropile and constitutes an important brain centre for the processing of sensory input, coordination of movement and navigation [20,21]. The highly conserved basic structure of the central complex, along with diverse specifications in response to ecological requirements among different insect species, make this brain structure a very interesting model for evolutionary developmental studies [3,10,20]. Between the two insect models *Drosophila* and *Tribolium* a temporal shift in the emergence of central complex neuropile was observed with *Tribolium* developing a functional larval central complex during embryogenesis whereas it develops only at the onset of adult life in *Drosophila* [3,10]. It is however not known how these temporal differences are established during development on a cellular and molecular level.

78 The entire insect central nervous system including the brain is produced by neural stem
79 cells, the neuroblasts (NBs) [22]. While there are evolutionary modifications in the relative
80 position of trunk NBs and their gene expression profiles between fly and beetle, the core
81 determinants specifying their role as neural progenitors are conserved [8]. NBs undergo
82 repeated divisions producing rows of ganglion mother cells (GMCs) which divide one more
83 time to produce neurons and/or glia (see Fig. 1, top panel). This leads to neural cell lineages
84 that include the neuroblast itself and its progeny [23,24]. Several NBs of the anterior-most
85 part of the neuroectoderm contribute to the central complex, which has been characterized
86 as the most complex brain structure (apart from the optic lobe) [25,26]. Intriguingly, in
87 *Drosophila* and in the grasshopper *Schistocerca gregaria* a neuroblast subtype, the type-II
88 neuroblasts (type-II NBs), were found to prominently contribute to the formation of the
89 central complex [27,28]. These specific neuroblasts generate more offspring by producing
90 another class of neural precursors, the intermediate progenitors (INPs), which also divide in
91 a stem cell like fashion [29,30] (Fig. 1, lower panel). Type-II NBs and INPs have attracted a lot
92 of attention because intermediate, cycling progenitors have also been described in
93 vertebrates, the radial glia cells, which produce a variety of cell types [31,32]. In addition, in
94 *Drosophila* brain tumours have been induced from type-II NB lineages [33], opening up the
95 possibility of modelling tumorigenesis in an invertebrate brain, thus making these lineages
96 one of the most intriguing stem cell model in invertebrates [34,35].
97

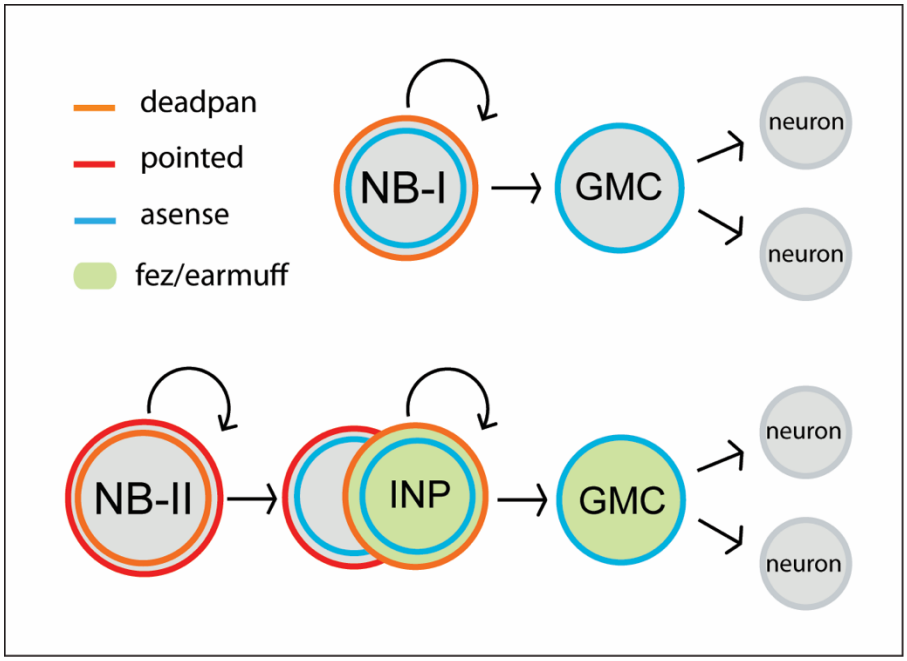

98

99 **Figure 1) Neuroblasts of the *Drosophila* nervous system.** Type-I neuroblasts (type-I NBs)
100 (top panel) and type-II neuroblasts (type-II NBs) (lower panel). Type-I NBs undergo stem-
101 cell-like divisions with each round producing a ganglion mother cell (GMC) that divides one
102 more time to produce two neurons or glia cells. In *Drosophila*, all type-I NBs express *dpn* and
103 *ase* whereas GMCs express only *ase*. Type-II NBs express *dpn* and *pnt* but not *ase*. They also
104 undergo repeated divisions, with each round producing an intermediate progenitor cell
105 (INP) which also is a proliferating progenitor and expresses *ase*. INPs undergo a maturation
106 process during which *pnt* is still expressed initially, but not *dpn*. Mature INPs express *dpn*,
107 *ase* and *fez/erm* whereas GMCs express *ase* and *fez/erm*. Type-II NB lineages are only found
108 in the anterior brain, they produce central complex neurons and glia [30,36].
109
110 In the developing insect brain the number of neurons that is produced by each type-II NB is
111 significantly larger than the offspring of a type-I NB. Medial *Drosophila* type-II NBs produce
112 an average of 450 neurons whereas type-I NBs of the brain only generate 100-200 neurons
113 each [37–39]. This increased number of neural cells that are produced by individual type-II
114 lineages along with the fact that neuroblast lineages can produce different types of neurons,
115 leads to the generation of extensive neural complexity within the anterior insect brain
116 [27,30].
117 Based on descriptions of large proliferative lineages in the grasshopper *Schistocerca*
118 *gregaria,* a hemimetabolous insect distantly related to flies, it is widely believed that type-II
119 NBs and INPs are conserved within insects [25,40]. However, a molecular characterisation of
120 such lineages that on the one hand will allow to test whether the cell type markers
121 characterized in *Drosophila* are more widely conserved, and on the other hand will facilitate
122 an identification of sub-cell types, has not been performed in an insect other than
123 *Drosophila*.
124 Whereas it is widely believed that *Tribolium* does use type-II NB in central complex
125 formation [3,17,41] their presence has so far not been unequivocally shown and a thorough
126 comparison of type-II NB lineages and their sub-cell-types between the fly and the beetle
127 model has been lacking.
128 The characterization of type-II NBs in *Drosophila* has in large parts been based on a specific
129 reporter line in which eGFP expression is driven by an *earmuff (fez/erm)* enhancer element
130 and marks INP-lineages [30,42,43]. *Tribolium earmuff* has been first described as *Tc-fez*,

131 referring to the vertebrate *earmuff* ortholog *fez* [19]. We will use *Tc-fez/erm* in the
132 following. A defined sequence of gene expression has been described in *Drosophila* type-II
133 NBs, INPs and GMCs. The ETS-transcription factor *pointed* (*pnt*) marks type-II NBs [44,45],
134 which do not express the type-I NB marker *asense* (*ase*) but the neural gene deadpan (*dpn*)
135 (Fig. 1). Intermediate progenitors express *fez/erm* and *ase* and at a more mature stage also
136 *dpn*, whereas *prospero* (*pros*) marks mature INPs and GMCs [30,46]. *Six4* is another marker
137 for *Drosophila* type-II NBs and INPs [47].
138 In the present work we characterize type-II neuroblasts in *Tribolium* with respect to their
139 number, their location and the conservation of the molecular markers known from
140 *Drosophila*. We also wanted to test, in how far the earlier emergence of the central complex
141 in beetles would be reflected by a change of division activity of type-II NBs or intermediate
142 progenitors. To that end, we used CRISPR-Cas9 induced genome editing for creating a *Tc-*
143 *fez/erm* enhancer trap line to characterize embryonic *Tc-fez/erm* -expressing cells including
144 INPs and GMCs of type-II NB lineages and combined this line with other labelling methods
145 including multicolour *hybridisation chain reaction* (HCR) [48,49]. We found that the
146 *Tribolium* embryo produces 9 *Tc-pnt*-expressing type-II NBs compared to only 8 type-II NB
147 lineages in the *Drosophila* embryo [50]. We show that these lineages produce central
148 complex cells and confirm a largely conserved molecular code that differentiates INPs of
149 distinct maturation stages and GMCs. Intriguingly, we found that lineage sizes in *Tribolium*
150 embryos are considerably larger and include more mature INPs than in the *Drosophila*
151 embryo [50]. We also show that the placodal marker gene *Tc-six4* characterizes the
152 embryonic tissue that gives rise to the larger anterior group of type-II NBs, whereas *Tc-six3*
153 is marking only an anterior subset of these lineages. Interestingly there is a part of the
154 central complex precursors expressing neither *Tc-six3* nor *Tc-otd,* which is absent from all
155 type-II NB lineages.
156
157 **Results**
158 **A CRISPR-Cas9-NHEJ generated enhancer trap lines marks *Tc-fez/erm*-expressing cells**
159 **at the embryonic and larval stage**
160 We created an enhancer trap line driving eGFP that reflects *Tc-fez/erm* gene expression in
161 the embryo. We named the line *fez magic mushrooms* (fez-mm-eGFP) because it marks the
162 mushroom bodies of the larval brain (Fig. 2 A-C). The reporter construct was inserted 160 bp

163 upstream of the *fez/erm*-transcription start site using the *non-homologous end joining*
164 (NHEJ) repair mechanism (see supplementary Fig. S1 for scheme). Enhancer traps
165 sometimes only reflect parts of a gene expression pattern, therefore we carefully evaluated
166 eGFP co-expression with *Tc-fez/erm*-RNA. We found that at the embryonic stage fez-mm-
167 eGFP co-localized with most *Tc-fez/erm*-expressing cells in an area that will give rise to the
168 protocerebral structures mushroom bodies, larval eyes and central complex [11,19] (Fig. 2,
169 panel D). The fez-mm-eGFP line marked several progenitor cell types including cells that we
170 characterize as type-II NB-derived intermediate progenitors (see below). Based on these
171 analyses, we use the fez-mm-eGFP expression as a reporter for *Tc-fez/erm* expression.
172

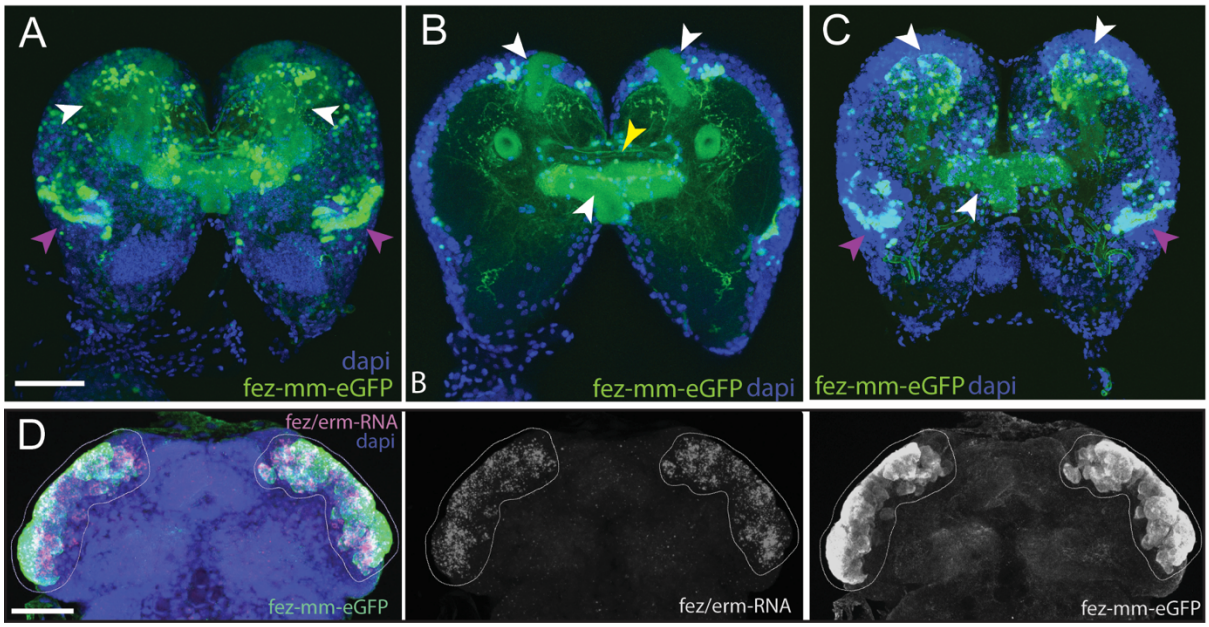

173

174 **Figure 2) Magic mushrooms (fez-mm-eGFP) reporter line.** A-C) eGFP-expression in a larval
175 instar brain, D) EGFP antibody labelling in combination with *Tc-fez/erm* RNA *in situ* in the
176 embryonic head, A-D) Dapi labelling of nuclei. Scalebars in A and D are 50 µm. **A)** Full
177 projection of whole brain scan (4th instar larvae): fez-mm-eGPF expression marks many cells
178 of the mushroom bodies (white arrowheads) and of the larval optic lobe (purple
179 arrowheads). Note that we use the terms dorsal and ventral with respect to the neuraxis of
180 the larva. See [10] for orientation. **B)** Central part of the whole brain scan (projection of
181 substack, same brain as in A): mm-eGFP marks the peduncles of the mushroom bodies
182 (white arrowheads) and some central complex ensheathing cells (probably glia cells; yellow
183 arrowhead). **C)** Projection of the dorsal part of same brain as in A shows calyces and
184 peduncles of mushroom bodies (white arrowheads), and optic neuropile (purple

185 arrowheads). **Panel D)** Extensive co-localization of fez-mm-eGFP with *Tc-fez/erm*-RNA in
186 white encircled area which gives rise to protocerebral structures. Projection of all planes
187 where expression was detected, embryonic stage NS11.
188
189 ***Tc-pointed* marks a population of nine type-II NBs that are associated with fez-mm-**
190 **eGFP marked INP-lineages**
191 To identify type-II NBs, we searched for cell groups that express the markers known from
192 flies. The transcription factor *pointed* (*pnt*) marks type-II NBs in *Drosophila* and is required
193 for their correct differentiation [44,45]. In both *Tribolium* and *Drosophila*, *pnt* is also
194 expressed in other areas (this work/[51,52]). Therefore, we looked for *Tc-pnt* expression in
195 large cells with large nuclei (typical NB morphology) that were closely associated with *Tc-*
196 *fez/erm*-expressing cells (marking putative INPs). We found a total of 9 such clusters instead
197 of the 8 expected from flies (Fig. 3 A-C). We also found that the large *Tc-pnt* expressing cells
198 as well as fez-mm-eGFP expressing cells are mitotically active (Fig. 3 C-I). Further molecular
199 and cell size analysis corroborated our interpretation that these cells constitute type-II NBs,
200 intermediate progenitors (INPs) at different maturation stages and ganglion mother cells
201 (GMCs) (see details below).
202 Looking at a series of embryonic stages we determined the emergence and further
203 development of *Tc-pnt* and fez-mm-eGFP expressing lineages as well as their arrangement
204 with respect to the embryonic head and to one another. We first detected conspicuous
205 adjacent expression of *Tc-pnt* and fez-mm-eGFP at stage NS7 (not shown). At stage NS11
206 seven *Tc-pnt*-clusters are present in a horse-shoe-shaped formation surrounding fez-mm-
207 eGFP positive cells (white arrows in Fig. 3 A, star marks one cluster out of focus). At stage
208 NS13 these groups are found in a position at the medial border of the head lobes and their
209 number has increased to nine. The seven clusters that were already present at stage NS11
210 are arranged in an anterior group (white arrowheads in Fig. 3B) at stage NS13 while two
211 additional clusters have emerged more posteriorly (yellow arrows in Fig. 3B-I). The clusters
212 are in different depths (reflected by the three optical sections shown in Fig. 3 B-I to B-III,
213 clusters out of focus are visualized by grey circles in Fig. 3 B'I-II, respectively). Fez-mm-eGFP
214 expression not related to type-II NB offspring was found in the lateral head lobe from NS13
215 onwards (blue arrowheads in Fig. 3). At stage NS14 six of the anterior-medial clusters are
216 aligned in one plane along the medial rim of the developing brain (Fig. 3 C-I), whereas the

217 most posterior cluster of the anterior group is located at a separate position and in a deeper
218 plane (Fig. 3C-II). The posterior group is found at about the same focal plane as well (Fig. 3
219 C-II). The aligned six clusters produce their *Tc-fez/erm*-positive offspring towards laterally
220 whereas the *Tc-fez/erm*-positive offspring of the more posterior cluster is found medially of
221 it (Fig. 3 C-II). The two most posterior clusters produce *Tc-fez/erm*-cells in an anterior-lateral
222 direction (Fig. 3 C-II). The apparent re-arrangement of the *Tc-pnt*-clusters from the anterior
223 rim of the embryonic head to a medial position reflects not active migration but follows the
224 overall tissue movements during head morphogenesis that was previously described in
225 *Tribolium* [19] (Fig. 3 D). Based on their position by the end of embryogenesis (stage NS14)
226 we assign the nine type-II NB clusters into two groups: one anterior median group consisting
227 of seven type-II NBs and one posterior group consisting of two type-II NBs (see Fig. 3 C and
228 D).

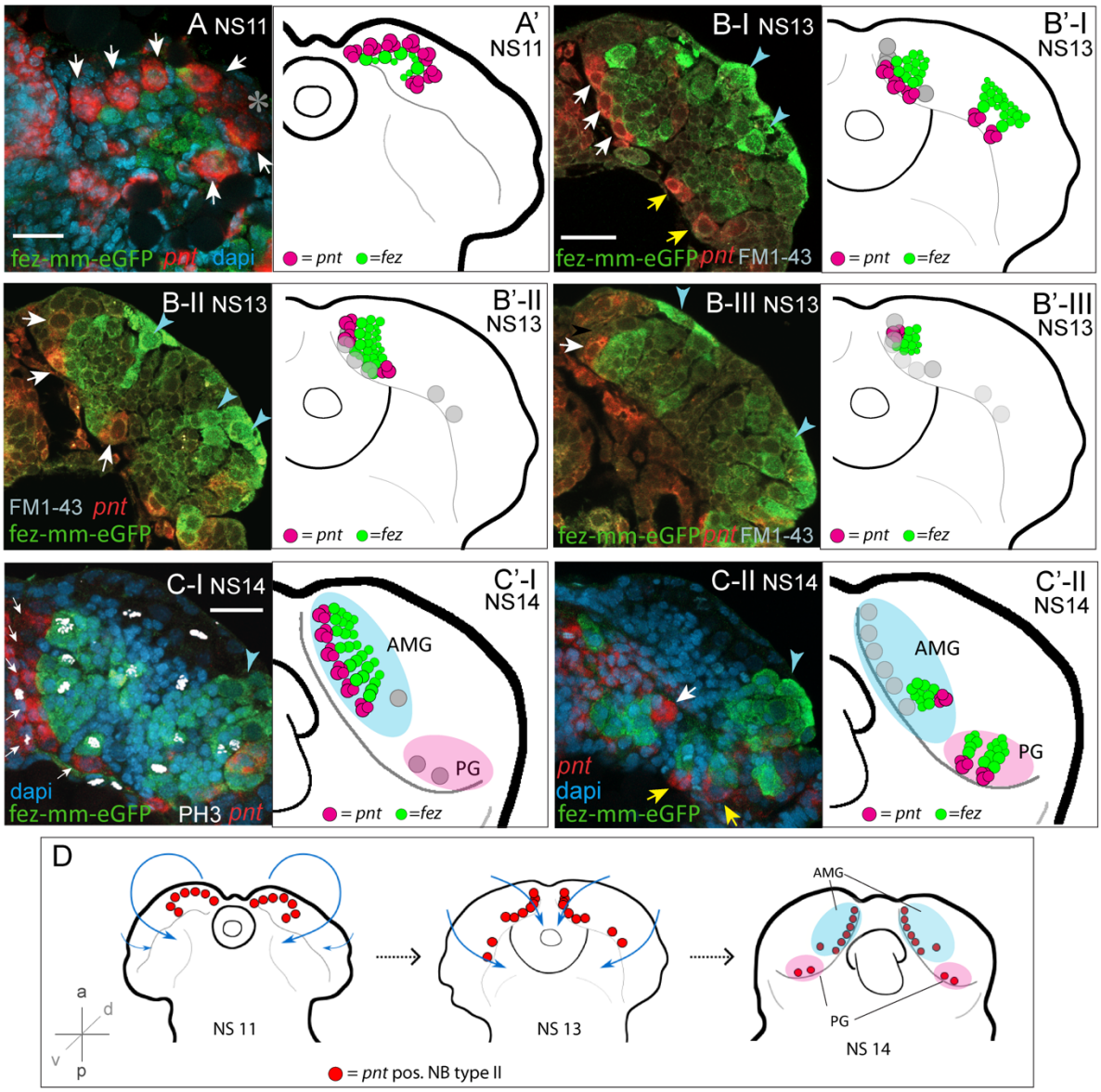

Figure 3) Developmental occurrence and progression of *Tc-pnt*-clusters and associated fez-mm-eGFP cells (type-II NB lineages). A-C) Anti-GFP antibody staining reflecting fez-mm-eGFP expression in combination with *Tc-pnt* RNA *in situ* hybridisation and dapi labelling of nuclei (A, C) or FM1-43 membrane staining (B), single planes from confocal z-stacks of right head lobes. Scalebars are 25 µm. A'-C') Schematic drawing of the head lobe at the respective stages; clusters out of focus depicted by grey circles. D) Schematic depiction of the localization of type-II NBs during *Tribolium* head morphogenesis. **A)** At stage NS11 seven *Tc-pnt*-clusters (white arrows) are found in an anterior-medial horseshoe-like arrangement with fez-mm-eGFP cells in the centre. Asterisk indicates the position of one *Tc-pnt*-cluster which is outside the focal plane of this image. **B)** At stage NS13 the seven anterior-medial clusters have been moved to the medial margin of the developing brain by

241 morphogenetic movements of the head lobes (white arrows). The clusters are situated in
242 different dorso-ventral levels shown in the different images B-I to B-III. Two additional
243 posterior *Tc-pnt*-clusters have appeared (yellow arrows). Blue arrows point to fez-mm-eGFP
244 positive cells that are not part of the type-II NB lineages. **B-I**: ventral level **B-II** mid-level, **B-**
245 **III**: dorsal level. **C)** At stage NS14 a group of six clusters are arranged in one plane anterior-
246 medially in the brain lobe (white arrows) (**C-I).** Anti-PH3 labelling marks mitotic cells within
247 the lineages (white signal) and clusters out of the focal plane are indicated by grey circles in
248 C'-I. **C-II** One cluster of the anterior median group (white arrow) is in a deeper plane, as well
249 as the two posterior clusters (yellow arrows). Blue arrowheads point to lateral fez-mm-eGFP
250 expression not associated with type-II NBs. A'-C') AMG =anterior medial group (blue), PG
251 =posterior group (pink). Grey circles in B'-C' indicate position of type-II NBs in different focal
252 planes. **D)** *Tc-pnt*-expressing cells identified as type-II NBs first appear bilaterally in the
253 anterior most part of the embryonic head (stage NS11). During head morphogenesis this
254 anterior tissue folds over so that the type-II NBs end up in a more medial position. Two
255 more type-II NBs emerge posteriorly (stage 13). At the end of embryogenesis (stage NS14)
256 the type-II NBs can be divided in an anterior medial group (AMG (blue); including type-II NBs
257 1-7, numbering starting from anterior) and a posterior group (PG (pink), including type-II
258 NBs 8-9).
259
260 **Characterization of cell- and nuclear size of *pnt*-positive type II NBs**
261 We wanted to confirm that each of the *Tc-pnt* and *Tc-fez/erm* expressing lineages contains a
262 neuroblast. Neuroblasts, including type-II NBs, are larger than other cells, have larger nuclei
263 and are mitotically active [40]. Therefore, we determined the cell size of the largest cells of
264 the *Tc-pnt* cluster and compared it to a random sample of cells of the embryonic head. Both
265 samples were taken from stage NS13 and NS14 embryos. We found that the cells that we
266 had assigned as Type-II NBs had a significantly larger diameter (av.: 12.98 µm; n=43) than
267 cells of the reference sample (av.: 6.75 µm; n=1579) (Fig. 4). We also found that the
268 diameters of nuclei of type-II NBs were significantly larger (av.: 8.73 µm; n=17) than the
269 ones of a control sample (av.: 5.21 µm; n=1080) (Fig. 4). Although type-II NBs were clearly
270 larger than the average cell of the head lobes the control sample also contained cells of an
271 equal size (figure 4) which may constitute type-I NBs.
272

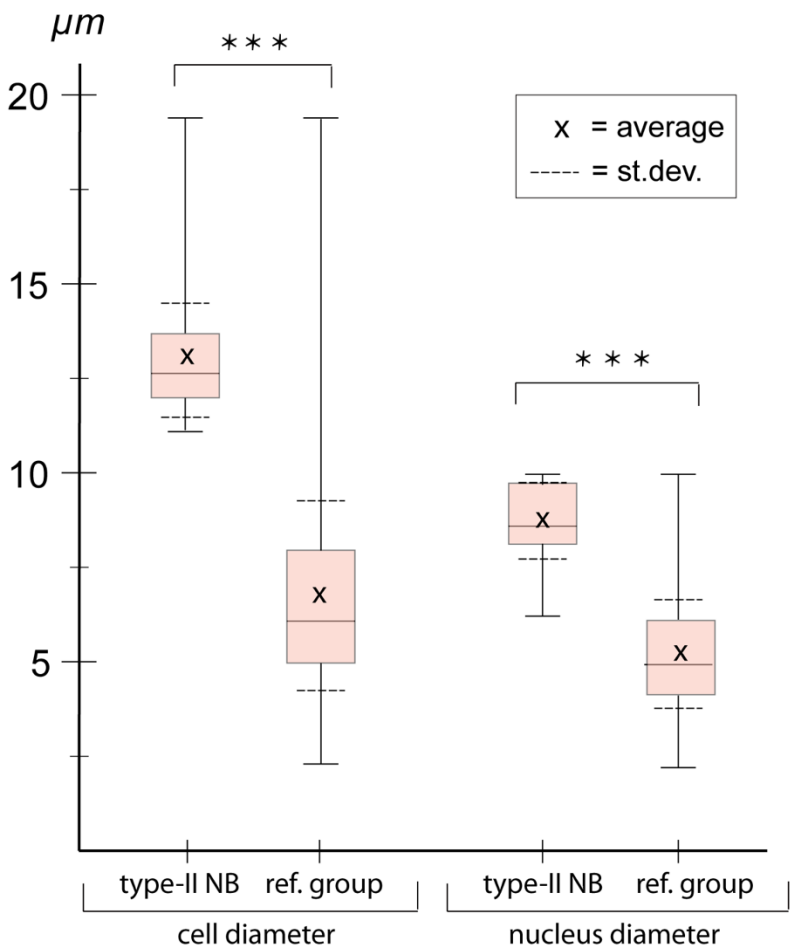

Figure 4) Cell- and nuclear diameter of type-II NBs compared to a control group. Stages NS13-14. Left: diameter of *Tc-pnt*-pos. type-II NBs (average diameter=12.98 µm; n=43) compared to control group (average diameter=6.75, n=1579). Right: average nuclear diameter of type-II NBs (=8,73 µm, n=17) compared to average nuclear diameter of control group (=5.21, n=1080). Differences between groups are significant (t-test; *** ≅ P < 0.001).

Conserved patterns of gene expression mark *Tribolium* type-II NBs, different stages of INPs and GMCs

Drosophila type-II NBs, INPs and GMCs express a specific sequence of genes including *asense* (*ase*), *deadpan* (*dpn*) and *prospero* (*pros*) (Fig. 1) [30]. However, these markers have up to now not been tested for expression in type-II lineages in other organisms. We tested if the respective lineages express these markers in a comparable sequence in the beetle and if they mark distinctive cell types within the lineages (Fig. 5 panel A-D and Fig. panel 6 A, B). We found that the large *Tc-pnt*-positive but fez-mm-eGFP negative cells (i.e. type-II NBs) express the gene *Tc-dpn*, in line with expression of this gene in *Drosophila* neural precursors

289 (Fig. 5, panel A). Like *Drosophila* type-II NBs, these cells do not express the type-I NB marker
290 *Tc-ase* (yellow arrowhead in Fig. 5, panel D). We further found additional cells directly
291 adjacent of the type-II NBs itself which we believe are recently born immature INPs. They
292 are *Tc-pnt*-positive but fez-mm-eGFP-negative and neither express *Tc-ase* (Fig. panel D, pink
293 arrowheads). Expression of *Tc-ase* starts in the following in immature *Tc-pnt*-positive INPs
294 (Fig. 5 panel D; blue arrowhead) and is maintained in INPs that are *Tc-pnt*-negative but are
295 marked by fez-mm-eGFP (Fig. 5, panel D and E). *Tc-dpn* is absent from immature *Tc-pnt*-
296 positive INPs (Fig. 5D, pink arrowhead) but is expressed in mature INPs (orange arrowheads
297 in Fig. 5, panel B). Cells that are located at the distal end of the lineages that do not express
298 *Tc-dpn* but are positive for fez-mm-eGFP and *Tc-ase* are classified as GMCs (Fig. 5, panels B,
299 C and E). We found the gene *Tc-pros* expressed in most fez-mm-eGFP expressing cells of a
300 lineage (in Fig. 6, panel A-B) and infer from the extent of the expression that it is expressed
301 in mature INPs (*Tc-dpn*+) and GMCs (*Tc-dpn*-). Fez-mm-eGFP positive cells at the base of the
302 lineage that do not express *Tc-pros* are immature INPs (Fig. 6, panel A, B; blue arrowheads).
303 In summary, the expression dynamics found in the *Tribolium* type-II NB lineages are very
304 similar to the one found in *Drosophila.* Therefore these neural markers can be used for a
305 classification of cell types within the lineages into type-II NBs (*Tc-pnt*+, *Tc-fez/erm*-, *Tc-ase*-,
306 *Tc-dpn*+, *Tc-pros*-), immature-I INPs (*Tc-pnt*+, *Tc-fez/erm*-, *Tc-ase-, Tc-dpn-, Tc-pros*-),
307 immature-II INPs (*Tc-pnt*+, *Tc-fez/erm*+, *Tc-ase*+, *Tc-dpn*-, *Tc-pros*-), mature INPs (*Tc-pnt*-, *Tc-*
308 *fez/erm*+, *Tc-ase*+, *Tc-dpn*+, *Tc-pros*+), and GMCs (*Tc-pnt*-, *Tc-fez/erm*+, *Tc-ase*+, *Tc-dpn-, Tc-*
309 *pros*+). This classification is summarized in Fig. 7 A-B. Image stacks from specimens co-
310 stained with the anti-PH3 mitosis marker (data shown in fig. 3C and listed in table 1 and 2,
311 available at https://doi.org/10.25625/8IVICL) indicate that immature-I and -II INPs are not
312 dividing whereas mature INPs are.
313

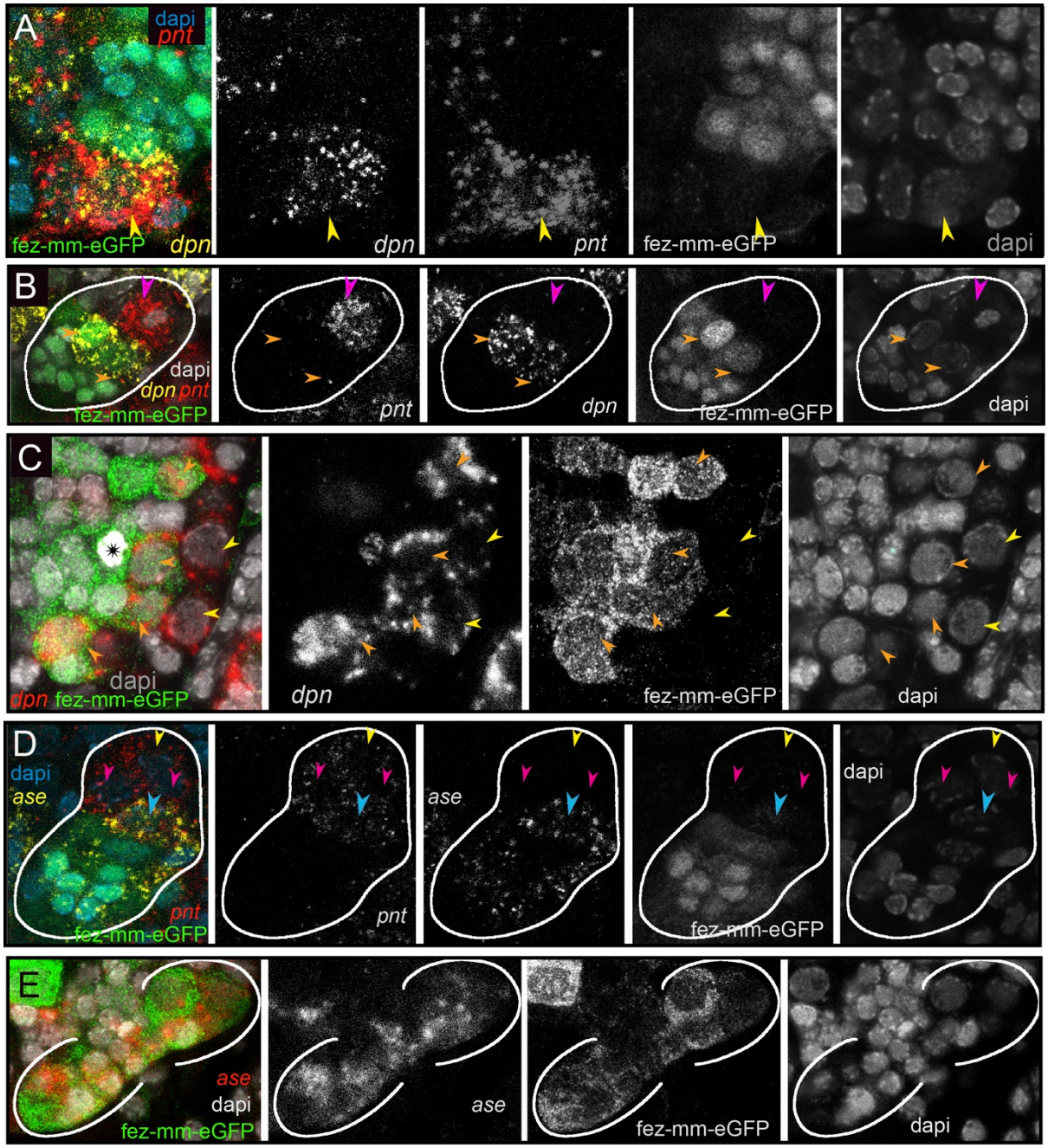

Figure 5: Differential expression of the neural markers *Tc-pnt, Tc-fez/erm, Tc-dpn* and *Tc-ase* in type-II NBs, INPs and GMCs. A, B, D) Anti-GFP staining visualizing fez-mm-eGFP expression in combination with HCR-labelling of further factors. C, E) GFP antibody staining in combination with RNA *in situ* hybridisation. A-E) Dapi staining of nuclei. All panels are single planes from confocal z-stacks. **Panel A)** Stage NS12, expression of *Tc-pnt* and *Tc-dpn* in type-II NBs (yellow arrowhead) with adjacent fez-mm-eGFP positive INPs. **Panel B)** Stage NS13, white line marks one lineage. Expression of *Tc-dpn* is absent in the immature-I *Tc-pnt*+ INPs (pink arrowhead) but present in mature INPs (orange arrowheads), white line marks one lineage. Type-II NB not in focus of this image. **Panel C)** Stage NS14, expression of

Tc-dpn in type-II NBs (yellow arrowheads), and mature INPs (orange arrowheads). Asterisk marks mitosis in a fez-mm-eGFP cell visible through the condensation of chromatin stained by dapi. **Panel D)** Stage NS13, *Tc-ase*- and *Tc-pnt*-expression in type-II NBs and INPs, white line marks one lineage. Yellow arrowhead: type-II NBs (*Tc-pnt*+), pink arrowheads: immature-I INP (*Tc-pnt*+), blue arrowhead: immature-II INP (*Tc-fez*+/ *Tc-ase*+/ *Tc-pnt*+). **Panel E)** Stage NS13, expression of *Tc-ase* in fez-mm-eGFP positive cells, location of type-II NBs and immature-I INPs is outside the focus.

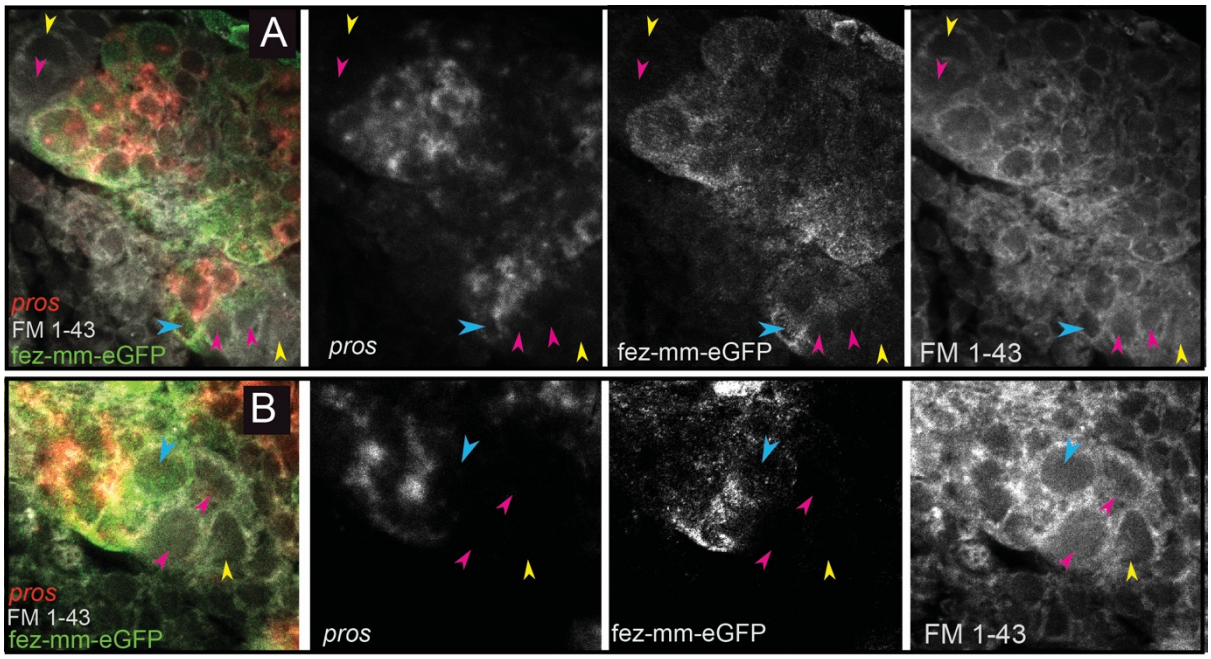

Figure 6) Expression of *Tc-pros* in fez-mm-eGFP cells. A-B) Anti-GFP antibody staining in combination with *Tc-pros* RNA *in situ* hybridization. Membranes stained with FM 1-43. Single planes from confocal z-stacks. **Panel A)** Stage NS13, two type-II NB lineages producing INPs and GMCs in opposing directions. Expression of *Tc-pros* in mature INPs and GMCs. Cluster of type-II NBs (yellow arrowheads) and immature-I INPs (pink arrowheads). Immature-II INPs express *Tc-fez/erm* but not *Tc-pros* (blue arrowhead). **Panel B)** Stage NS13, detail of *Tc-pros*-negative type-II NBs (yellow arrowhead) and immature-I INPs (pink arrowheads) and immature-II INP (blue arrowhead). Note that distinction between type-II NB and immature INPs in **A)** and **B)** is only made based on position.

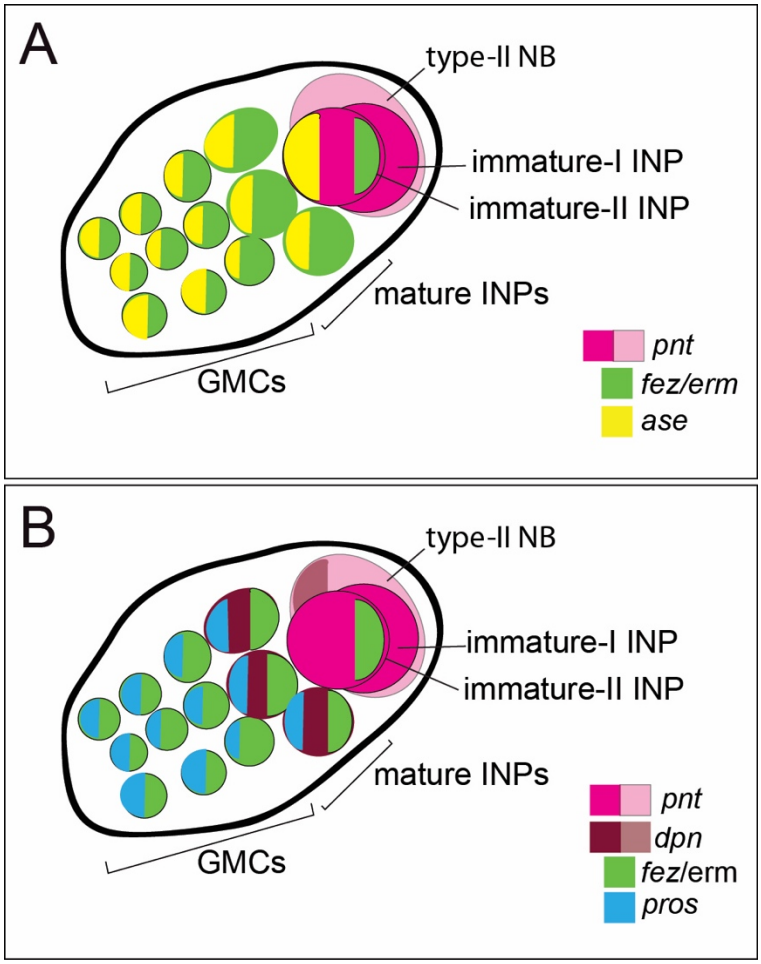

Figure 7) Schematic drawing of expression of different markers in a type-II NB lineage. A) and B) show the same lineage with *Tc-fez/erm* and *Tc-pnt* expression but with different additional markers mapped on top. **A)** Subclassification into type-II NBs (*Tc-pnt+*), immature-I INPs (*Tc-pnt+*), immature-II INPs (*Tc-pnt+, Tc-fez/erm+, Tc-ase+*) and mature INPs and GMCs (*Tc-fez/erm+, Tc-ase+*) (based on stainings shown in Fig. 5). **B)** Type-II NB (*Tc-pnt+, Tc-dpn+*), immature-I (*Tc-pnt+*) and immature-II (Tc-pnt+, *Tc-fez/erm+*). Mature INPs express *Tc-dpn*, *Tc-pros* and *Tc-fez/erm* whereas GMCs express only *Tc-fez/erm* and *Tc-pros* (based on staining shown in Fig. 5 and 6). Note that of the selected markers immature-I INPs express *Tc-pnt* only.

Type-II NB lineages produce central complex cells that are marked by shaking hands (skh)

To test if the *Tribolium* embryonic type-II NB lineages contribute to the beetle central complex like in the fly, we used the shaking hands- (skh-) reporter line that marks central complex neurons and their postmitotic embryonic precursors [41]. By co-staining for *Tc-pnt* and *Tc-fez/erm* RNA in the background of the skh-line we found that the skh-positive cells

364 are located directly distally of the type-II NB lineages in a position where the type-II NBs
365 derived neural cells are expected (Fig. 8 panels A-B, E,F). Most skh-cells have switched off
366 *fez/erm*-expression, but at the transition between *Tc-fez/erm* and skh cells we found some
367 cells that express both markers (Fig. 8 panel D, E), supporting the view that many skh-
368 positive central complex cells stem from the *fez*-expressing GMCs of the type-II NB lineages
369 (Fig. 8 E). We found skh cells at the end of lineages of the anterior-median group (Fig. 8,
370 panel A) and at the end the two posterior lineages (Fig. 8, panel B). We therefore conclude
371 that both groups contribute to central complex neuropile (Fig. 8 F). We cannot say whether
372 the lineage of type-II NB seven, which we assigned to the anterior-median group, but which
373 is located with some distance to the other type-II NB of that group (Fig. 3 C, D; grey circle in
374 Fig. 8 F), produces skh+ cells, but we assume that it does.
375

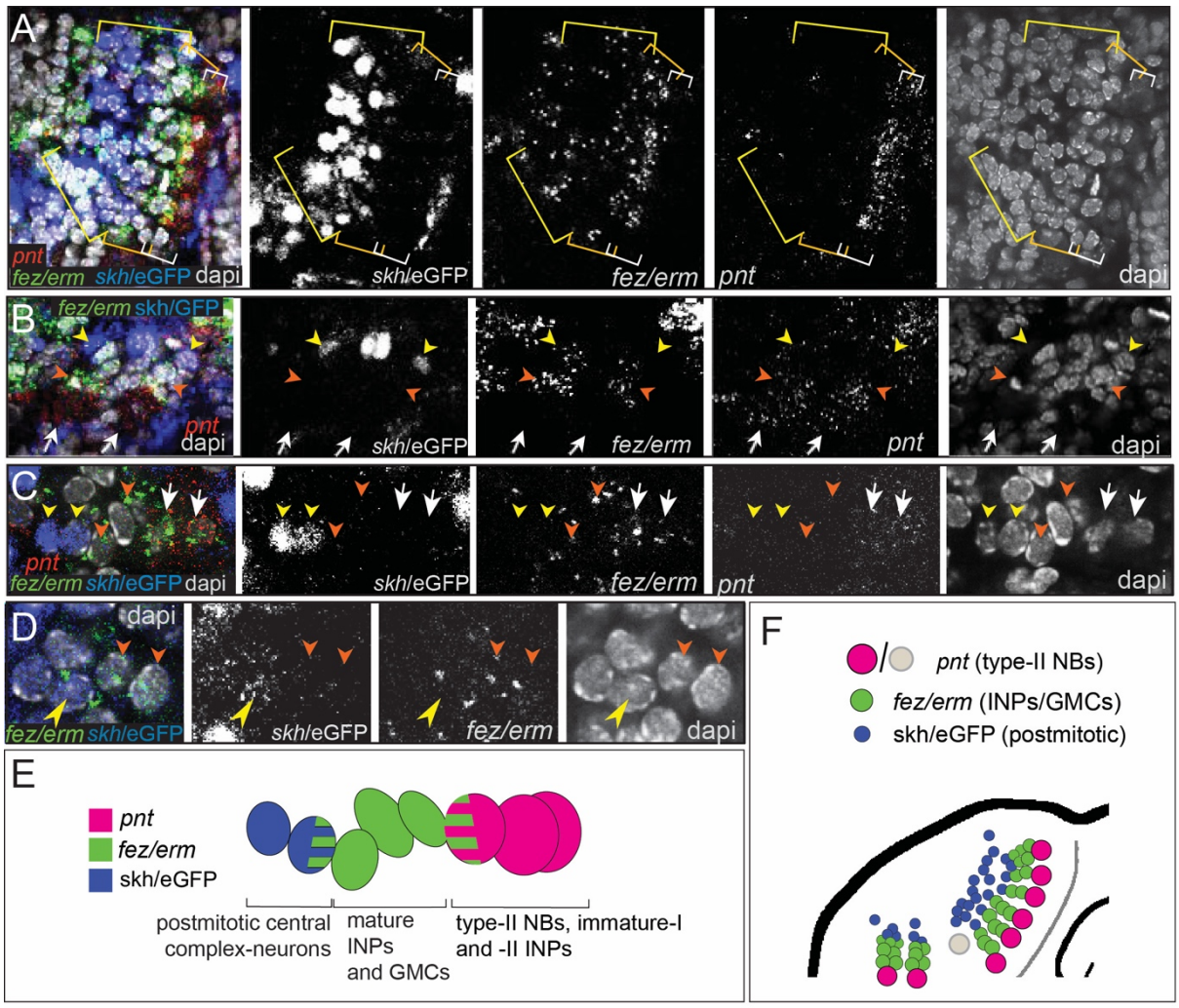

376
377 **Figure 8) Expression of the transgenic central complex reporter skh/eGFP in relation to**
378 **type-II NB lineages.** A-D) Antibody labelling of eGFP, which is expressed in the pattern of

379 skh [41] in combination with HCR visualizing *Tc-fez/erm* and *Tc-pnt*, dapi labelling of nuclei,
380 single planes of confocal z-stacks, all stage NS14. **A)** Left head lobe, anterior group of *Tc-pnt*-
381 positive type-II NBs, *Tc-fez/erm*-expressing INPs/GMCs and skh/eGFP positive postmitotic
382 cells. **B)** Left head lobe, posterior group of type-II NB lineages. *Tc-pnt+* type-II NBs or
383 immature-I/-II INPs (white arrows), *Tc-fez/erm*+ INPs/GMCs (orange arrowheads) and
384 skh/eGFPpostmitotic cells (yellow arrowheads). **C)** Detail of one lineage including type-II NB
385 cluster (*Tc-pnt*+, white arrows), INPs/GMCs (*fez+,* orange arrowheads) and skh/eGFPcells at
386 the end of the lineage (yellow arrowheads). **D)** Detail of transition from *Tc-fez/erm*+ cells
387 (orange arrowheads) to skh/eGFPcells reveals a small area of co-expression of both factors
388 (yellow arrowhead). **E)** Schematic drawing of type-II NB lineage showing relative positions
389 and markers of type-II NBs, INPs/GMCs and postmitotic central complex forming cells. **F)**
390 Schematic overview of the arrangement of the type-II NB lineages including skh/eGFP+
391 central complex forming cells in the head lobe of stage NS14 (immature-I/-II INPs not shown
392 for simplicity). No data on skh-GFP expression in lineage of type-II NB 7 (marked in grey) is
393 available.
394
395 **The *Tribolium* embryonic lineages of type-II NBs are larger and contain more mature INPs**
396 **than those of *Drosophila***
397 In beetles, a single-unit central body (most likely constituting the fan-shaped body [10])
398 develops during embryogenesis and has gained functionality at the onset of larval life [15].
399 By contrast, in *Drosophila* central complex commissural tracts originating from type-II NBs
400 form in the embryo but the type-II NB become quiescent and only resume divisions in the
401 late larval stage [29,50]. In stark contrast to *Tribolium* a functional central complex is only
402 observed in the adult fly [3]. In addition, the volume of the L1 central brain including the
403 central complex is about four times larger in *Tribolium* than it is in *Drosophila* [53], while
404 there are only small differences in the relative neuropilar volumes of the adult beetle and fly
405 central bodies [53,54]. As type-II NBs contribute to central complex development we asked
406 in how far the embryonic division pattern of these lineages in the beetle would reflect this
407 heterochronic development. To assess the size of the embryonic type-II NB lineages in
408 beetles we counted the *Tc-fez/erm* positive (fez-mm-eGFP) cells (INPs and GMCs) of the
409 anterior medial group (type-II NB lineages 1-7). As we were not always able to distinguish
410 between cells belonging to neighbouring INP-lineages we quantified and averaged the cell

411 number of all lineages of the anterior medial group. We also evaluated the proportion of
412 dividing cells in that group based on anti-PH3 staining (table 1).
413
414 **Table 1: *Tc-fez/erm* positive cell number (type-II NBs, INPs and GMCs)**

Embryo#/stage	*Total number of cells of 7 anterior lineages*	*% dividing cells (PH3 antibody)*	*Cells per lineage (average)*
1/NS 13	146	8.2%	20.9
2/NS 13	111	6.3%	15.9
3/NS 14	139	5.0%	19.9
4/NS 14	96	10.5%	13.7

415
416 We found that at stage NS13 (early retracting embryo) each lineage consisted on average of
417 18,4 progenitor cells and at stage NS14 (retracted embryo) of 16.8 progenitors. Between 5-
418 10 % of the cells were marked by the PH3 antibody. As PH3 marks dividing cells in a specific
419 phase, the portion of dividing cells may be higher. We further quantified the number of
420 mature *Tc-dpn*-positive INPs (table 2).
421
422 **Table 2: Mature INPs (*Tc-fez/erm* and *Tc-dpn* positive)**

Embryo #/ stage	*Total number of mature INPs of 7 anterior lineages*	*% dividing cells (PH3 antibody)*	*Number of mature INPs per lineage (average)*
1/NS 13	24	n.d.	3,4
2/NS 13	12	n.d.	1,7
3/NS 13	23	n.d.	3,3
4/NS 14	27	3,7%	3,9
5/NS 14	30	13,3%	4,3

423
424 We used the numbers from *Tribolium* (table 1, 2) for comparison with type-II NB lineages
425 from *Drosophila* embryos (data from [29]). At fly embryonic stage 13, which is comparable
426 to *Tribolium* stage NS14 in that is represents a retracted germband, lineages only contained
427 one or more INPs but no GMCs [29]. Therefore, we compared our data for the anterior
428 lineages of *Tribolium* stages NS13 and NS14 to the anterior and median cluster in the
429 *Drosophila* stage 15 and 16 embryos. In both species these stages are the two penultimate
430 stages of embryogenesis when all type-II NB lineages are present, and importantly, in
431 *Drosophila* the maximum lineage sizes and numbers of INPs are reached at these stages. We
432 found that the beetle lineages were significantly larger than the corresponding ones in
433 *Drosophila* (Fig. 9; *Drosophila* data taken from [29]). Of note, cell counts in *Drosophila* also
434 included neurons [29]. Our counts are based on *Tc-pnt* and fez-mm-eGFP expression and
435 therefore mostly included progenitors. However, based on the small area of co-expression

436 of *Tc-fez/erm* and skh-expression (see above/ figure 8) they may also include some newly
437 born neurons, but the counts in *Drosophila* included more mature neurons which further
438 increases the difference in the number of progenitor cells between the two species and the
439 observed difference in lineage size represents a minimum estimate.
440 Due to a lower quality of the image data from the posterior group which is in a deeper layer
441 (see Fig. 3) we were not able to quantify cells of this cluster in *Tribolium* . In *Drosophila,* the
442 posterior lineages are larger (av. 10 cells [29]) than the anterior and median ones, but they
443 are still smaller than the anterior lineages of *Tribolium* at the stages that were investigated.
444 We also found that the embryonic type-II NB lineages in *Tribolium* comprised significantly
445 more mature INPs (*Tc-dpn+/ Tc-fez+*) than the corresponding lineages in *Drosophila* (Fig. 9).
446 The described observations on the higher numbers of progenitor cells in *Tribolium* when
447 compared to *Drosophila* correlate with a previously described earlier (i.e. embryonic)
448 formation of a functional central complex in beetles, which is present in the first larval stage
449 [3].
450
451

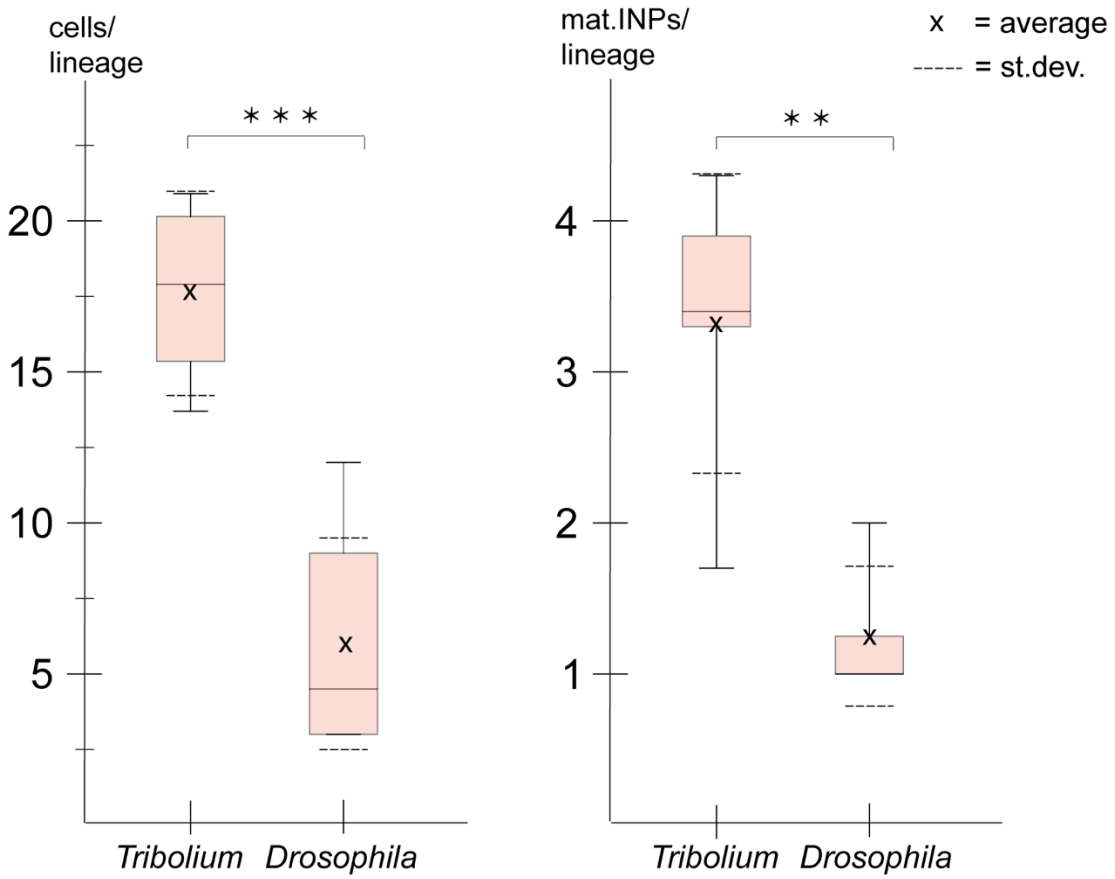

452
453

454 **Figure 9) Size comparison of *Tribolium* and *Drosophila* type-II NB lineages.** Anteriormedian
455 lineages from *Tribolium* stages 13 and 14 (quantified in this work, see table 1 and 2)
456 compared to *Drosophila* stages 15 and 16 (pooled data from [29]). Left: Lineage sizes
457 comprising type-II NBs, INPs and GMCs (*Tribolium* n=4; *Drosophila* n=8). Right: Number of
458 *Tc-dpn*-positive mature INPs (*Tribolium* n=5; *Drosophila* n=8). T-test p-value significance
459 level (t-test; *** ≅ P < 0.001, ** ≅ P < 0.01).
460
461 **Type-II NBs and their lineages are differentially marked by the head patterning**
462 **transcription factors *Tc-six4* and *Tc-six3* but do not express *Tc-otd***
463 The anterior-most embryonic insect head is divided into different territories by highly
464 conserved developmental transcription factors that give rise to different parts of the
465 protocerebrum [11]. Hence, we wondered in which of these molecular territories subsets of
466 type-II NB lineages are located, as neuroectoderm regionalization genes are candidates for
467 giving specific spatial identities to individual lineages. We tested co-expression with the
468 previously characterized head patterning transcription factors *Tc-otd*, *Tc-six4*, *Tc-six3*,
469 known to be active in the developing protocerebrum (*Tc-otd*) and in the anterior medial
470 region of the neuroectoderm, where type-II NBs emerge (*Tc-six3*, *Tc-six4*) [11,19,55,56]. We
471 found no co-expression of fez-mm-eGFP marked cells of both the anterior medial and
472 posterior lineages with *Tc-otd*. Rather, *Tc-otd* was expressed in the surrounding embryonic
473 head tissue. *Tc-otd* was also absent from the type-II NBs themselves (Fig. 10 panel A-B).
474 However, *Tc-otd* might be expressed in neural cells derived from these lineages as we can
475 detect expression in the central area of the brain lobes where for instance skh cells are
476 located (Fig. 8 panel A, F; Fig. 10 panel A-B). Interestingly, we found that *Tc-six4* is expressed
477 specifically in that area of the head lobe in which the type-II NBs clusters 1-6 of the anterior
478 medial group first differentiate. At stage NS13 *Tc-six4* marks both, type-II NBs and fez-mm-
479 eGFP expressing INPs and some surrounding cells (Fig. 11, panel A). At the following
480 differentiation stage (NS14) *Tc-six4* still marks the type-II NBs clusters of the anterior medial
481 group but is not expressed in the fez-mm-eGFP INPs (Fig. 11 panel B). It is also not
482 expressed in the posterior group of type-II NBs but only marks type-II NBs of the anterior
483 medial group. Finally, we found that *Tc-six3* marks, and is restricted to, the anterior-most
484 lineages 1-4 including both the type-II NBs and the fez-mm-eGFP marked INPs/GMCs (Fig. 11
485 panel C). These results reveal candidates for distinguishing type-II identity from type-I NBs in

486 the brain. Only the latter is possibly marked by *Tc-otd* as *Drosophila otd* is expressed in type-
487 I brain neuroblasts [57]. By contrast, *Tc-six4* only marks type-II NBs and appears to be an
488 early determinant of the anterior medial group. *Tc-six4* is also a candidate for distinguishing
489 the anterior medial from the posterior cluster. The results also reveal a subdivision of the
490 anterior cluster by *Tc-six3*, which marks the four most anterior type-II NBs.
491

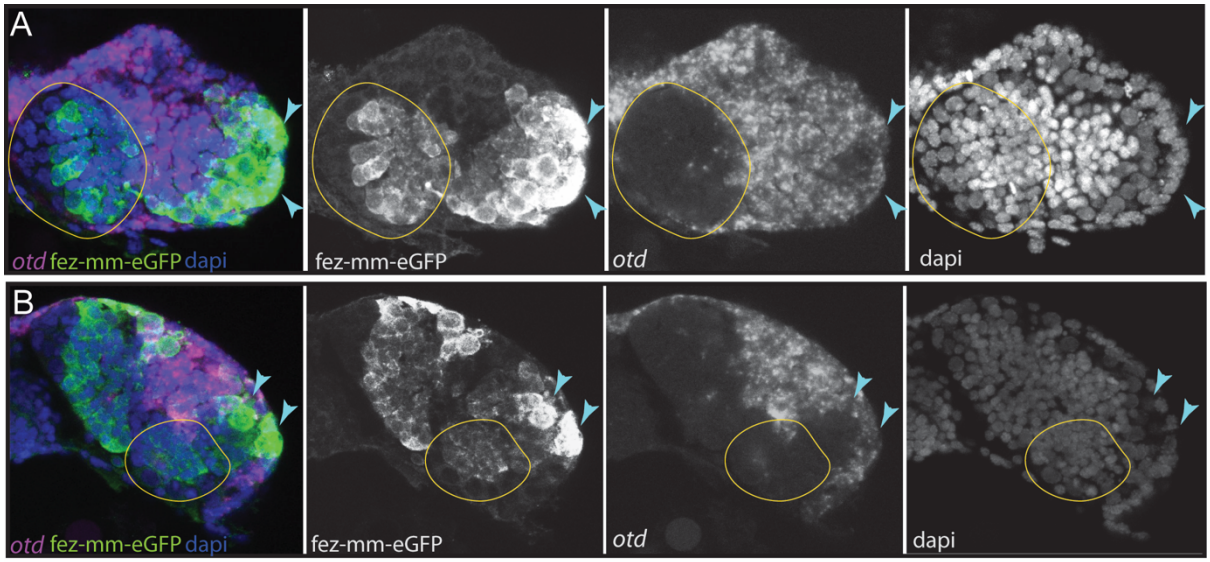

492

493 **Figure 10) Expression of *Tc-otd* in relation to the fez-mm-eGFP lineages**. A/B) RNA *in situ*
494 hybridisation for *Tc-otd* in combination with GFP antibody staining and dapi labelling of
495 nuclei, A and B show projections of different levels of NS14 embryos, right head lobe. **A)** *Tc-*
496 *otd* is neither expressed in type-II NBs nor the in the fez-mm-eGFP positive INPs of the
497 anterior medial group (both positioned within encircled area) but it is expressed in the
498 directly surrounding tissue. **B)** Likewise, *Tc-otd* is not expressed in type-II NBs or fez-mm-
499 eGFP cells of the posterior group (encircled area). A lateral area of *Tc-fez/erm* and *Tc-otd* co-
500 expression (**A/B**, blue arrow) likely is part of the eye anlagen [19].
501

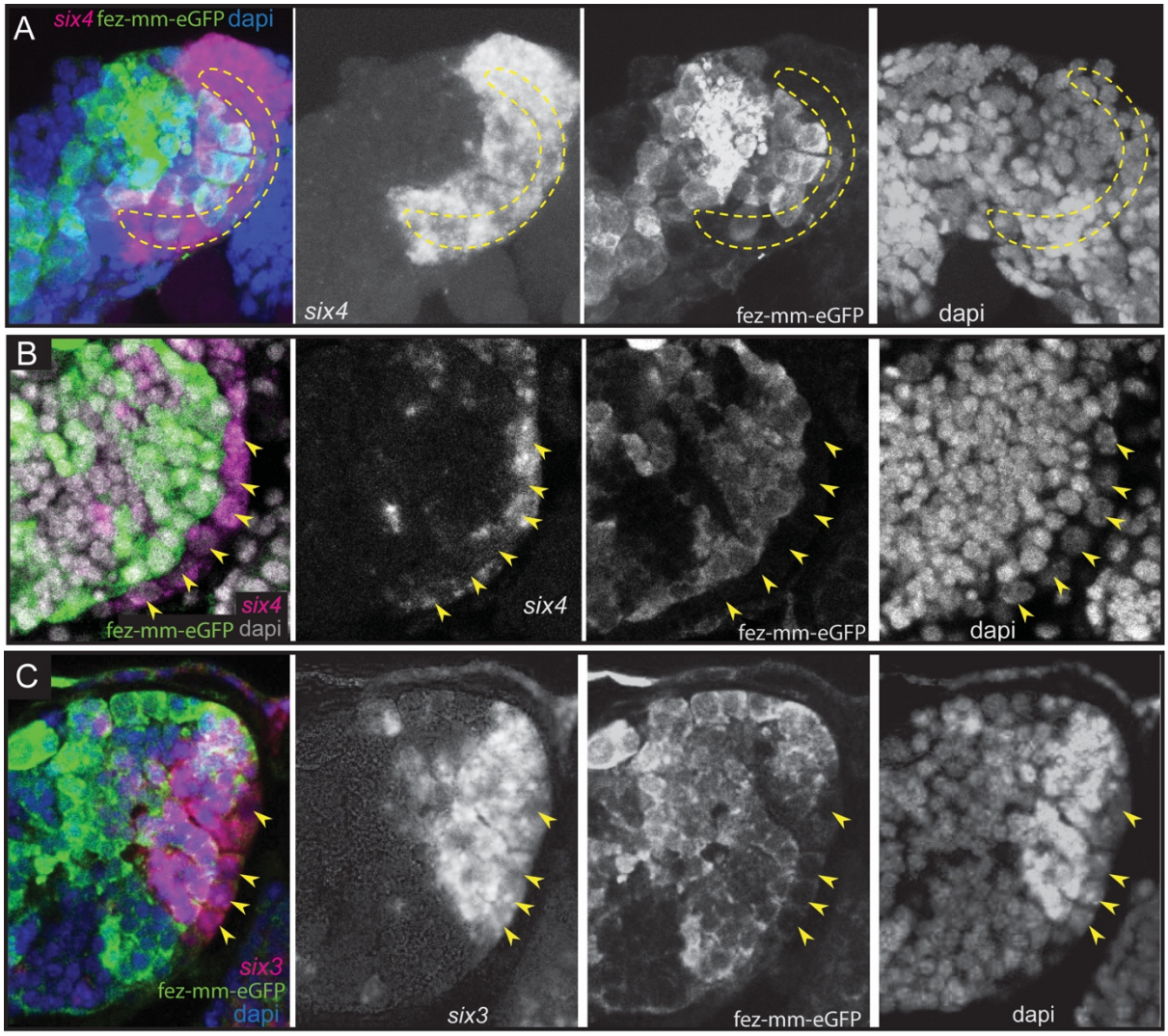

Figure 11) Expression of *Tc-six4* and *Tc-six3* in type-II NBs and INPs. A-C) RNA *in situ* hybridisations of *Tc-six4* and *Tc-six3* in combination with GFP antibody staining reflecting fez-mm-eGFP expression, dapi labelling of nuclei, left head lobes shown. **Panel A)** Stage NS13; *Tc-six4* is expressed in an area encompassing type-II NBs (positioned in encircled area) and mm-eGFP expressing INPs. **Panel B)** Stage NS14; *Tc-six4* is now restricted to type-II NBs and their youngest progeny that do not express fez-mm-eGFP (yellow arrowheads). **Panel C)** Stage NS14; *Tc-six3* specifically marks the four anterior-most lineages. It is expressed in the type-II NBs at the base of the lineages (yellow arrowheads) and in the fez-mm-eGFP positive INPs and possibly also in GMCs. It is absent from the remaining lineages of the anterior medial group and is also not seen in the posterior group (not shown).

Discussion

516 **Evolutionary divergence of number and grouping of embryonic type-II NB lineages**
517 **between beetle, fly and grasshopper**
518 We have identified a total of 9 type-II NB lineages on each side of the *Tribolium* embryonic
519 head. This represents a major evolutionary divergence as in both, the hemimetabolan
520 grasshopper *Schistocerca gregaria* and the fruit fly *Drosophila melanogaster* only 8
521 embryonic type-II NBs were identified [29,38]. Our finding of an additional type-II NB lineage
522 at the embryonic stage shows that the number of type-II NBs is not fixed across insects and
523 suggests that evolutionary divergence in brain development between species may be driven
524 by differences in the number of progenitor lineages. To test this, further research is
525 required to determine where the additional lineage in *Tribolium* is located and if it is
526 associated with morphological differences of the brain.
527 Although in the frame of this work we did not perform lineage tracing we can speculate
528 about which NB might be lacking in fly embryos based on our data. In the hemimetabolan
529 *Schistocerca* there is no obvious clustering of type-II NBs, and they are all arranged in one
530 row at the medial rim of the head lobes. In *Tribolium* we have observed an arrangement of
531 the type-II NBs into two groups per side, one large anterior medial group containing seven
532 type-II NB clusters and one posterior group of two type-II NBs. The anterior six of the
533 anterior medial group are arranged in one row like in the grasshopper. In *Drosophila* there
534 are three described groups referred to as the anterior, the middle and the posterior cluster
535 [29]. The posterior cluster consists of two type-II NBs and therefore most likely corresponds
536 to the posterior two type-II NBs in *Tribolium*. The *Drosophila* middle and anterior cluster are
537 most likely equivalent to the anterior medial group of *Tribolium.* However, the type-II NB 7,
538 which we assigned to the anterior medial group, but which is a bit separated and produces
539 offspring into the opposite direction (see Fig. 2 C-II, white arrow) might be the one that does
540 not have a homologue in the fly embryo. The identification of more specific spatial markers
541 for type-II NBs (in addition to *Tc-six3* and *Tc-six4*) or lineage tracing tools are required to
542 identify the neuroblast, which is not present in fly embryos. Subsequently, it would be
543 especially interesting to see what the role of the additional type-II NBs in the beetle is and
544 which neuropile it contributes to.
545 Summing up, there is a tendency towards grouping of type-II NBs into subsets in the
546 holometabolan models that was not observed in the only hemimetabolan studied so far. A
547 ninth type-II NB was only found in the *Tribolium* embryo represents a striking

548 developmentally divergent feature, but its role and the homologisation of individual type-II
549 NBs between the different insects requires further studies.
550
551 **Gene expression identifies homologous cell types and suggests conservation of gene**
552 **function between fly and beetle type-II NB lineages**
553 The genes defining the different stages of differentiation in type-II NB lineages have been
554 identified and intensively studied in *Drosophila,* but it had remained unclear, in how far the
555 respective patterns and mechanisms were conserved. Our results show a large degree of
556 conservation of expression and probably also function – at least in holometabola. We
557 identified type-II NBs by their larger than average size [40] and the expression of the
558 signature marker *Tc-pnt* adjacent to a group of *Tc-fez/erm* expressing cells (INPs and GMCs).
559 In *Drosophila* both these factors have key functions in defining the developmental potential
560 of type-II NBs and INPs: Pnt suppresses Ase in type-II NBs and promotes the formation of
561 INPs [45]. Loss of *pnt* expression leads to a de-differentiation of INPs as *fez/erm* is no longer
562 repressed in young INPs [44]. Fez/Erm controls proliferation of INPs by activating Pros and
563 prevents dedifferentiation of INPs into type-II NBs [43]. We show that also in *Tribolium* INPs
564 undergo a maturation process, during which expression of *Tc-pnt* stalls and expression of
565 *Tc-fez/erm* is switched on. Despite both factors characterising different stages of INP
566 maturation they are not completely mutual exclusive and we observed a small window of
567 overlap in immature-II INPs, highly suggestive of a conserved role of Pnt in the activation of
568 *fez/erm* [44] (Fig. 12). *Drosophila dpn* is a neural marker [58] expressed in type-II NBs and
569 again in mature INPs, leaving a gap of expression in immature-I and II INPs. *Drosophila ase* is
570 repressed in type-II NBs but expressed together with *fez*/*erm* in INPs and GMCs where its
571 expression overlaps with *pros* [59]. We found identical dynamics of gene expression in
572 *Tribolium* (see Fig. 12) suggesting conservation of gene function within the lineages and a
573 conserved process of INP maturation.
574 In conclusion, expression of the genes examined in this study in type-II NBs and their
575 lineages is highly conserved in fly and beetle, which is implicit of conserved gene function
576 and a conserved process of central complex formation.
577

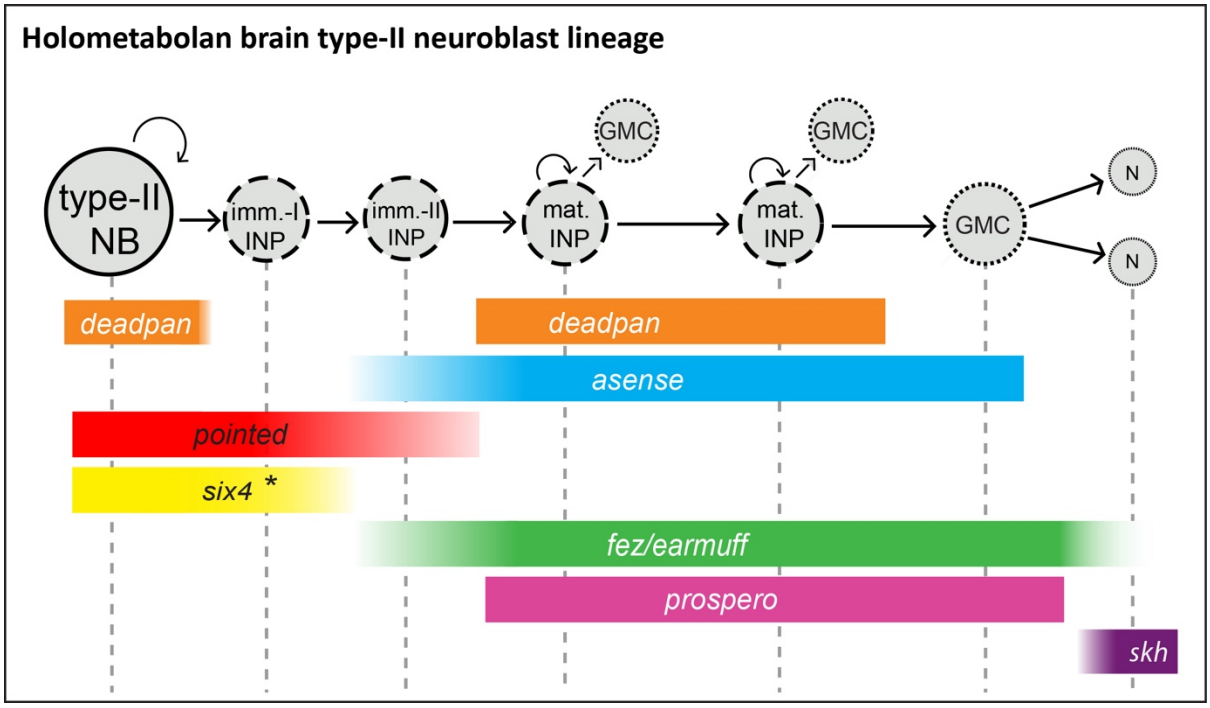

Figure 12) Conserved aspects of gene expression in type-II NB lineages of the holometabolan models *Drosophila* and *Tribolium*. Overview on the different cell types within one lineage (type-II NBs, INPs, GMCs and central complex neurons), their mitotic activity, and summary of the expression of key factors in the respective cell types. INPs are divided into immature-I, immature-II, and mature INPs with each subtype having a unique expression profile. Note that each lineage can have several mature INPs. We strongly assume that glia are also produced from these lineages in *Tribolium*, as they are in *Drosophila* [30]. * In the *Tribolium* embryo *Tc-six4* is only expressed in the anterior medial lineages, and its expression is overlapping with *Tc-fez/erm* at an earlier stage (NS12) whereas it is restricted to type-II NBs and immature-I INPs, mutually exclusive with *Tc-fez/erm*, at a later embryonic stage (NS14). *Drosophila six4* was found in all 8 larval lineages [47]. The scheme is based on this work and [30,41,43,44,47]. NB= neuroblast; imm.-I/-II INP = immature-I/-II intermediate progenitor; mat. INP= mature intermediate progenitor; N=neuron; skh=shaking hands (enhancer trap) [41].

Divergent timing of type-II NB activity and heterochronic development of the central complex

Previous work described a heterochronic shift in central complex formation between fly and beetle [3,10]. In *Tribolium* parts of the central complex develop during embryogenesis. It becomes functional at the onset of the first larval stage, and is presumably required for the

599 more complex movements of the beetle larvae using legs [3]. In both *Drosophila* and
600 *Tribolium* the anterior groups of type-II NBs (anterior medial group of *Tribolium* and anterior
601 and middle cluster of *Drosophila*) are fully present in the last 3rd of embryogenesis, with the
602 beginning of germ band retraction [8,29,60]. However, in the *Drosophila* embryo only a
603 limited number of INPs and GMCs are produced before they enter a resting stage prior to
604 hatching [29]. By contrast, we show that *Tribolium* type-II NB lineages are much larger at the
605 embryonic stage compared to *Drosophila* [29]. They also include more mature, *Tc-dpn*
606 expressing cycling INPs which have the capability of driving the increase in lineage size. We
607 believe that this increased activity may contribute to the embryonic development of a
608 functional central body and protocerebral bridge [3]. This hypothesis does however require
609 further confirmation by lineage tracing experiments and by testing how manipulating
610 central genes acting within the lineages will affect the timing of central complex
611 development. In addition, differences in cell number in the individual central complex
612 neuropiles between *Tribolium* and *Drosophila* have to be assessed, as the higher number of
613 progenitors may also reflect a higher number of neurons present in the adult beetle fan
614 shaped body or may be due to a slower rate of division and a resulting accumulation of
615 progenitor cells. Lastly, we do not yet have any information whether *Tribolium* type-II NBs,
616 or *Tribolium* neuroblasts in general, also enter a stage of quiescence at the end of
617 embryogenesis as they do in *Drosophila* [29] and what role neurons born in the 1st larva play
618 in *Tribolium*.
619 Another emerging question is if and when *Tribolium* type-II NB lineages are active during
620 larval development and how that relates to the described steps of central complex
621 development. After preformation in the embryo *Drosophila* type-II NBs have their main
622 period of activity in the 3rd larva and the lineages are much larger and contain more INPs
623 than the *Tribolium* embryonic lineages [30]. Therefore, it would be interesting to see if type-
624 II NB lineages are present and active in the late larval brain of *Tribolium*.
625 Taken together, we have for the first time identified and molecularly characterized
626 embryonic type-II NBs and INPs as the major central complex progenitor pool in an insect
627 outside *Drosophila*. We have observed quantitative differences within these lineages when
628 compared between *Tribolium* and *Drosophila*. Based on these findings we hypothesize that
629 increased division behaviour of type-II NB lineages is required for the embryonic central
630 complex development as found in beetles. Our findings set the basis for future work on the

631 relationship of the identified type-II NB lineages and the timing of central complex
632 development.
633
634 **The placodal marker *Tc-six4* may be responsible for the differentiation and the spatial**
635 **identity of the anterior medial group of type-II NBs**
636 The different type-II NB lineages contribute to different parts of the brain. For instance, only
637 the anterior four type-II NB lineages form the w, x, y, and z tracts of the central complex in
638 flies and grasshoppers. Hence, there must be signals that make them different despite the
639 conserved and well-studied sequence of neural gene expression and functional interactions
640 in *Drosophila* (Fig. 12) [30,43,44,59]. In the ventral nerve cord, the different identities of the
641 NBs are specified by the combination of spatial patterning genes expressed in the
642 neuroectoderm at the time of delamination [24]. However, little is known about these
643 signals for type-II NBs. In *Tribolium* the domains of head patterning genes in the brain
644 neuroectoderm are well characterized and some highly conserved territories like the
645 anterior-medial *six3*-positive domain were described and suggested to give respective NBs
646 different spatial identities [11,19,55]. The *Tc-six4* expression domain is also largely
647 coincident with an embryonic structure termed insect head placode, a neurogenic,
648 invaginating tissue [56,61] potentially homologous to the vertebrate adenohypophyseal
649 placode which is also marked by *six4* [11,56]. A placodal origin of *Drosophila* type-II NBs has
650 been shown for one type-II NB, and it is assumed that the other type-II NBs also stem from
651 placodal tissue [29,50,62].
652 *Tc-six4* is also a very interesting factor with regards to the specification of type-II NBs
653 because it is expressed only in the anterior group of type-II NBs. Hence, it could contribute
654 to distinguishing their developmental fate from the posterior group. This is however
655 different in the *Drosophila* larva. Here Six4 is expressed in all eight lineages where it
656 prevents the formation of supernumerary type-II NBs and a premature differentiation of
657 INPs [47]. In the *Tribolium* embryo Six4 may have a similar rate limiting role within the
658 anterior group of type-II NBs. However, its early expression in a small part of the
659 neuroectoderm [56] and the delamination of the anterior-medial type-II NB group within
660 this domain also hints at an instructive role of *Tc-six4* in the formation of the anterior medial
661 group.
662

663 ***Tc-six3* marks a subset of type-II NBs whereas *Tc-otd* is absent from all lineages**

664 Importantly, we found that in *Tribolium* late embryogenesis, *Tc-six3* is expressed specifically
665 within the lineages of type-II NBs 1-4 of the anterior medial group, but not in the other
666 linages. In grasshopper and fly these anterior 4 lineages (DM1-4) give rise to the z, y, x and
667 w tracts [25,38] and contribute crucially to the development of protocerebral bridge and
668 central body. These tracts form a major midline crossing neuropile of the central body which
669 serves as a scaffold in the development of this structure [3,25]. We conclude that in
670 *Tribolium* the evolutionary ancient *six3* territory gives rise to the neuropile of the z, y, x and
671 w tracts. This might well be the same in other insects such as flies and grasshoppers but has
672 to our knowledge not been looked at in detail in these models. In the beetle the central
673 body is also missing in weak *Tribolium Tc-six3*-RNAi phenotypes, suggesting that *Tribolium*
674 *six3* is required for the formation of this structure [19]. Given that central complex neuropile
675 is marked by additional factors such as *Tc*-foxQ2 (*Drosophila* fd102c [63]) and *Tc-rx*- [3,17], it
676 would be interesting to see the relationship of additional spatial patterning genes with
677 regards to the type-II NB lineages in future studies.

678 The gene *otd* is a marker of the posterior protocerebrum and *six3* and *otd* are believed to
679 subdivide the embryonic anterior brain into two major domains [55]. This subdivision is also
680 part of the recently revisited concept of an ancestral division of the insect protocerebrum
681 into archicerebrum (*six3*-positive) and prosocerebrum (*otd*-positive) [11]. As discussed
682 above, *Tc-six3* is expressed in the anterior-most four type-II NB lineages, but unexpectedly,
683 we found that *Tc-otd* is specifically absent from all type-II NB lineages, suggesting that its
684 inhibition is required for the development of all these lineages. Interestingly, the lineages of
685 type-II NB 5 and 6 (and presumably of type-II NB 7) of the anterior cluster and the posterior
686 type-II NB lineages do neither express *Tc-otd* nor *Tc-six3* showing that there are
687 protocerebral structures expressing none of these conserved markers in development,
688 questioning the assigned generalized role of these two factors in subdividing the
689 protocerebrum [11,55] .

690 In summary, our findings are just the beginning of the quest for the genes required for the
691 identity specification of type-II NB lineages. The genes known to be involved in head
692 patterning are an excellent starting point for this purpose [11,18].

693

694 **Methods**

695

696 **Creation of transgenic reporter line**

697 Using CRISPR-Cas9 we have inserted a transgene into the *Tc-fez/erm* locus that includes
698 *egfp* behind the *Tribolium* basal heat shock promoter (bhsp68), which is not active by itself
699 but can be activated by nearby enhancer elements [64,65]. The transgene also contained
700 the coding sequence of Cre-recombinase (not used in this work) transcribed from the same
701 promoter, and the eye pigmentation gene *Tc-vermilion* behind the eye-specific 3xP3
702 enhancer element [66] (see Fig. S1 A for map of the transgene). On the repair plasmid the
703 transgene was flanked by CRISPR target sequences derived from *Dm-yellow* and *Dm-ebony*,
704 which were used for *in vivo* linearisation of the transgene.

705 Using CRISPR Optimal Target Finder [67] we designed three guide RNAs (gRNAs) targeting
706 the genomic region 2.5 kb upstream of the *Tc-fez/erm* transcription start site (see table S1).
707 We produced three plasmids where single gRNAs were transcribed from the *Tribolium* pU6b
708 RNA promoter, as described in [12]. We co-injected the three gRNAs plasmids at 125µg/µl
709 each, gRNAs targeting the *Dm-yellow* and *Dm-ebony* sequence at 125µg/µl each, Cas9
710 helper plasmid (see [12]) at 500 µg/µl and the repair plasmid at 500 µg/µl. Embryos of the
711 white eyed *Tribolium vermilion-white* (*vw*) strain (G0) were injected, raised and then bred to
712 *vw*-beetles in individual crosses. The offspring of these crosses (F1) were screened for black
713 eyed heterozygous carriers of the transgene. These were again outcrossed to *vw*-beetles
714 and the heterozygous offspring (F2) were further analysed genetically (see table S2) and
715 with respect to fluorescent signal. Siblings of the F2 generation were then crossed to one
716 another to generate the homozygous line (fez-mm-eGFP). Details of the insertion can be
717 found in Fig. S1 A.

718 We also used the shaking hands (skh) enhancer trap line (G10011-GFP) which marks central
719 complex cells [41].

720

721 **Larval brain dissection, fixation, and staining**

722 Larval brains of the newly generated *Tc-fez/erm* enhancer trap line fez-mm-eGFP were
723 dissected and stained as described in [16]. Brains were mounted in *Vectashield* for
724 microscopic inspection. See table S4 for a list of antibodies and staining reagents used.

725

726 **Embryonic RNA *in situ* hybridisation, hybridisation chain reaction and antibody staining**

727 Gene identifiers and primer sequences that were used for amplification can be found in
728 table S3. The fragments were inserted into a pJet1.2 cloning vector. Standard RNA *in situ*
729 probes were synthesised using the 5X Megascript T7 kit (Ambion) according to the
730 manufacturers protocol. Embryo fixation and single colour RNA *in situ* chain reaction in
731 combination with antibody staining to eGFP or phospo-histone H3 staining to mark mitoses
732 was conducted as described in [68]. Embryos were also stained for DNA (dapi) or cell
733 membranes (FM1-43). A full list of antibodies and staining reagents can be found in table S4.
734 Probes for multicolour *hybridisation chain reaction (HCR)* binding *Tc-fez/erm*, *Tc-dpn*, *Tc-ase*
735 and *Tc-pnt* were produced by Molecular Instruments (see table S5). Labelling reactions were
736 performed as described in [69]. Antibody staining to eGFP was performed following the
737 completion of the HCR staining (see [68]). All embryos were mounted in *Vectashield* for
738 microscopic inspection (see table S4).
739
740 **Image acquisition and analysis**
741 Multichannel image stacks were recorded using a Zeiss LSM 980 confocal laser scanning
742 microscope. Image stacks consisted of 100-300 slices, depending on the specimen. The
743 resolution ranged from 1024 x 1024 to 2048 x 2048 pixels. Plane thickness was optimized
744 according to width of the pinhole and ranged from 0.1 – 1 µm. We used FIJI [70] for 3
745 dimensional inspection, to export individual planes or to generate maximum intensity
746 projections. Cropping and adjustment of brightness and contrast was done with GIMP
747 (version 2.10.32) or Adobe Photoshop CS5.
748
749 **Evaluation and of cell size and cell number**
750 Cell and nuclear diameters of type-II NBs and a control group were measured based on the
751 image stacks using FIJI [70] across 7 embryos. Lineage size and numbers of mitoses (based
752 on *Tc-pnt* and *fez*-mm-eGFP expression/ anti-PH3 staining) was evaluated by manual
753 counting based on image stacks derived from 4 head lobes of 4 embryos (≧ 28 anterior-
754 medial lineages). The number of *Tc-dpn* expressing intermediate progenitors was evaluated
755 in the same way across 5 embryos (≧ 35 anterior-medial lineages). Reference data on
756 *Drosophila* lineage size (type-II NBs, INPs, GMCs and neurons) and numbers of *dpn*-
757 expressing intermediate INPs were extracted from [29]. Statistics on all numerical data
758 (standard deviations and two-tailed t-tests) were performed using Microsoft Excel 2016.

759

760 **References**

761

762 1. Konstantinides N, Kapuralin K, Fadil C, Barboza L, Satija R, Desplan C. Phenotypic
763 Convergence: Distinct Transcription Factors Regulate Common Terminal Features. Cell.
764 Elsevier Inc.; 2018;174:622-635.e13. https://doi.org/10.1016/j.cell.2018.05.021
765 2. Li X, Chen Z, Desplan C. Temporal Patterning of Neural Progenitors in Drosophila. Curr Top
766 Dev Biol. 2014;8:1385–95. https://doi.org/10.1016/B978-0-12-396968-2.00003-8
767 3. Farnworth MS, Eckermann KN, Bucher G. Sequence heterochrony led to a gain of
768 functionality in an immature stage of the central complex: A fly–beetle insight [Internet].
769 PLoS Biol. 2020. http://dx.doi.org/10.1371/journal.pbio.3000881
770 4. Couto A, Wainwright JB, Morris BJ, Montgomery SH. Butterfly brain evolution. Curr Opin
771 Insect Sci. Elsevier Inc; 2020;42:55–60. https://doi.org/10.1016/j.cois.2020.09.002
772 5. Hakeemi MS, Ansari S, Teuscher M, Weißkopf M, Großmann D, Kessel T, et al. Screens in
773 fly and beetle reveal vastly divergent gene sets required for developmental processes. BMC
774 Biol. BMC Biology; 2022;20:1–13. https://doi.org/10.1186/s12915-022-01231-4
775 6. Klingler M, Bucher G. The red flour beetle T. castaneum: elaborate genetic toolkit and
776 unbiased large scale RNAi screening to study insect biology and evolution. Evodevo. BioMed
777 Central; 2022;13:1–11. https://doi.org/10.1186/s13227-022-00201-9
778 7. Tautz D, Friedrich M, Schröder R. Insect embryogenesis - What is ancestral and what is
779 derived? Development. 1994;120:193–9.
780 https://doi.org/10.1242/dev.1994.Supplement.193
781 8. Biffar L, Stollewerk A. Conservation and evolutionary modifications of neuroblast
782 expression patterns in insects. Dev Biol. Elsevier; 2014;388:103–16.
783 http://dx.doi.org/10.1016/j.ydbio.2014.01.028
784 9. Biffar L, Stollewerk A. Evolutionary variations in the expression of dorso-ventral
785 patterning genes and the conservation of pioneer neurons in Tribolium castaneum. Dev Biol.
786 Elsevier; 2015;400:159–67. http://dx.doi.org/10.1016/j.ydbio.2015.01.025
787 10. Koniszewski N, Kollmann M, Bigham M, Farnworth M, He B, Büscher M, et al. The insect
788 central complex as model for heterochronic brain development—background, concepts, and
789 tools. Dev Genes Evol. Development Genes and Evolution; 2016;226:209–19.
790 http://dx.doi.org/10.1007/s00427-016-0542-7
791 11. Posnien N, Hunnekuhl VS, Bucher G. Gene expression mapping of the neuroectoderm
792 across phyla – conservation and divergence of early brain anlagen between insects and
793 vertebrates. Elife. 2023;12:1–30. https://doi.org/10.7554/eLife.92242
794 12. Gilles AF, Schinko JB, Averof M. Efficient CRISPR-mediated gene targeting and transgene
795 replacement in the beetle Tribolium castaneum. Development. 2015;142:2832–9.
796 http://dev.biologists.org/cgi/doi/10.1242/dev.125054
797 13. Gilles AF, Schinko JB, Schacht MI, Enjolras C, Averof M. Clonal analysis by tunable
798 CRISPR-mediated excision. Dev. 2019;146:1–8. 10.1242/dev.170969
799 14. Posnien N, Schinko J, Grossmann D, Shippy TD, Konopova B, Bucher G. RNAi in the red
800 flour beetle (Tribolium). Cold Spring Harb Protoc. 2009;4:1–7. doi:10.1101/pdb.prot5256
801 15. Farnworth MS, Eckermann KN, Ahmed HM, Mühlen DS, He B, Bucher G. The red flour
802 beetle as model for comparative neural development: Genome editing to mark neural cells
803 in Tribolium brain development. Methods Brain Dev. 2020. https://doi.org/10.1007/978-1-
804 4939-9732-9_11

805 16. Hunnekuhl VS, Siemanowski J, Farnworth MS, He B, Bucher G. Immunohistochemistry
806 and Fluorescent Whole Mount RNA In Situ Hybridization in Larval and Adult Brains of
807 Tribolium. Methods Mol Biol. 2020. p. 233–51. https://doi.org/10.1007/978-1-4939-9732-
808 9_13
809 17. He B, Buescher M, Farnworth MS, Strobl F, Stelzer E, Koniszewski NDB, et al. An
810 ancestral apical brain region contributes to the central complex under the control of foxQ2
811 in the beetle tribolium. Elife. 2019;8:1–29. https://doi.org/10.7554/eLife.49065
812 18. Posnien N, Schinko JB, Kittelmann S, Bucher G. Genetics, development and composition
813 of the insect head - A beetle's view. Arthropod Struct Dev. Elsevier Ltd; 2010;39:399–410.
814 http://dx.doi.org/10.1016/j.asd.2010.08.002
815 19. Posnien N, Koniszewski N, Hein H, Bucher G. Candidate gene screen in the red flour
816 beetle tribolium reveals six3 as ancient regulator of anterior median head and central
817 complex development. PLoS Genet. 2011;7. https://doi.org/10.1371/journal.pgen.1002416
818 20. Honkanen A, Adden A, Da Silva Freitas J, Heinze S. The insect central complex and the
819 neural basis of navigational strategies. J Exp Biol. 2019;222.
820 https://doi.org/10.1242/jeb.188854
821 21. Pfeiffer K, Homberg U. Organization and functional roles of the central complex in the
822 insect brain. Annu Rev Entomol. 2014;59:165–84. https://doi.org/10.1146/annurev-ento-
823 011613-162031
824 22. Hartenstein V, Stollewerk A. The evolution of early neurogenesis. Dev Cell. Elsevier Inc.;
825 2015;32:390–407http://dx.doi.org/10.1016/j.devcel.2015.02.004
826 23. Doe CQ, Skeath JB. Neurogenesis in the insect central nervous system. Curr Opin
827 Neurobiol. 1996;6:18–24. https://doi.org/10.1016/S0959-4388(96)80004-3
828 24. Stollewerk A. A flexible genetic toolkit for arthropod neurogenesis. Philos Trans R Soc B
829 Biol Sci. 2016;371. https://doi.org/10.1098/rstb.2015.0044
830 25. Boyan GS, Reichert H. Mechanisms for complexity in the brain: Generating the insect
831 central complex. Trends Neurosci. Elsevier Ltd; 2011. p. 247–57. 10.1016/j.tins.2011.02.002
832 26. Strausfeld NJ. Arthropod Brains: Evolution, functional elegance, and historical
833 significance. The Belknap Press of Harvard University Press; 2012.
834 27. Boyan GS, Reichert H. Mechanisms for complexity in the brain: Generating the insect
835 central complex. Trends Neurosci. Elsevier Ltd; 2011;34:247–57.
836 http://dx.doi.org/10.1016/j.tins.2011.02.002
837 28. Boyan G, Liu Y, Khalsa SK, Hartenstein V. A conserved plan for wiring up the fan-shaped
838 body in the grasshopper and Drosophila. Dev Genes Evol. Development Genes and
839 Evolution; 2017;227:253–69. https://doi.org/10.1007/s00427-017-0587-2
840 29. Walsh KT, Doe CQ. Drosophila embryonic type II neuroblasts: Origin, temporal
841 patterning, and contribution to the adult central complex. Dev. 2017;144:4552–62.
842 https://doi.org/10.1242/dev.157826
843 30. Bayraktar OA, Doe CQ. Combinatorial temporal patterning in progenitors expands neural
844 diversity. Nature. Nature Publishing Group; 2013;498:449–55.
845 https://doi.org/10.1038/nature12266
846 31. Malatesta P, Appolloni I, Calzolari F. Radial glia and neural stem cells. Cell Tissue Res.
847 2008;331:165–78. https://doi.org/10.1007/s00441-007-0481-8
848 32. Barry DS, Pakan JMP, McDermott KW. Radial glial cells: Key organisers in cns
849 development. Int J Biochem Cell Biol. Elsevier Ltd; 2014;46:76–9.
850 http://dx.doi.org/10.1016/j.biocel.2013.11.013
851 33. Caussinus E, Gonzalez C. Induction of tumor growth by altered stem-cell asymmetric

852 division in Drosophila melanogaster. Nat Genet. 2005;37:1125–9.
853 https://doi.org/10.1038/ng1632
854 34. Homem CCF, Knoblich JA. Drosophila neuroblasts: A model for stem cell biology. Dev.
855 2012;139:4297–310. https://doi.org/10.1242/dev.080515
856 35. Bowman SK, Rolland V, Betschinger J, Kinsey KA, Emery G, Knoblich JA. The Tumor
857 Suppressors Brat and Numb Regulate Transit-Amplifying Neuroblast Lineages in Drosophila.
858 Dev Cell. 2008;14:535–46. 10.1016/j.devcel.2008.03.004
859 36. Southall TD, Brand AH. Neural stem cell transcriptional networks highlight genes
860 essential for nervous system development. EMBO J. 2009;28:3799–807.
861 https://doi.org/10.1038/emboj.2009.309
862 37. Bello BC, Izergina N, Caussinus E, Reichert H. Amplification of neural stem cell
863 proliferation by intermediate progenitor cells in Drosophila brain development. Neural Dev.
864 2008;3. https://doi.org/10.1186/1749-8104-3-5
865 38. Boyan G, Williams L. Embryonic development of the insect central complex: Insights
866 from lineages in the grasshopper and Drosophila. Arthropod Struct Dev. Elsevier Ltd;
867 2011;40:334–48. http://dx.doi.org/10.1016/j.asd.2011.02.005
868 39. Izergina N, Balmer J, Bello B, Reichert H. Postembryonic development of transit
869 amplifying neuroblast lineages in the Drosophila brain. Neural Dev. 2009;4:1–13.
870 https://doi.org/10.1186/1749-8104-4-44
871 40. Boyan G, Williams L, Legl A, Herbert Z. Proliferative cell types in embryonic lineages of
872 the central complex of the grasshopper Schistocerca gregaria. Cell Tissue Res.
873 2010;341:259–77. https://doi.org/10.1007/s00441-010-0992-6
874 41. Garcia-Perez NC, Bucher G, Büscher M. Shaking hands is a homeodomain transcription
875 factor that controls axon outgrowth of central complex neurons in the insect model
876 Tribolium. Development. 2021. https://doi.org/10.1242/dev.199368
877 42. Pfeiffer BD, Jenett A, Hammonds AS, Ngo TTB, Misra S, Murphy C, et al. Tools for
878 neuroanatomy and neurogenetics in Drosophila. Proc Natl Acad Sci U S A. 2008;105:9715–
879 20. https://doi.org/10.1073/pnas.080369710
880 43. Weng M, Golden KL, Lee CY. dFezf/Earmuff Maintains the Restricted Developmental
881 Potential of Intermediate Neural Progenitors in Drosophila. Dev Cell. Elsevier; 2010;18:126–
882 35. http://dx.doi.org/10.1016/j.devcel.2009.12.007
883 44. Xie Y, Li X, Deng X, Hou Y, O'Hara K, Urso A, et al. The Ets protein Pointed prevents both
884 premature differentiation and dedifferentiation of Drosophila intermediate neural
885 progenitors. Development. 2016;143:3109–18.
886 http://dev.biologists.org/lookup/doi/10.1242/dev.137281
887 45. Zhu S, Barshow S, Wildonger J, Yeh L, Jan Y. Ets transcription factor Pointed promotes
888 the generation of intermediate neural progenitors in Drosophila larval brains.
889 2011;108:20615–20. https://doi.org/10.1073/pnas.111859510
890 46. Bayraktar OA, Boone JQ, Drummond ML, Doe CQ. Drosophila type II neuroblast lineages
891 keep Prospero levels low to generate large clones that contribute to the adult brain central
892 complex. Neural Dev. 2010;5. https://doi.org/10.1186/1749-8104-5-26
893 47. Chen R, Hou Y, Connell M, Zhu S. Homeodomain protein Six4 prevents the generation of
894 supernumerary Drosophila type II neuroblasts and premature differentiation of
895 intermediate neural progenitors. PLoS Genet. 2021.
896 http://dx.doi.org/10.1371/journal.pgen.1009371
897 48. Choi HMT, Schwarzkopf M, Fornace ME, Acharya A, Artavanis G, Stegmaier J, et al. Third-
898 generation in situ hybridization chain reaction: Multiplexed, quantitative, sensitive,

899 versatile, robust. Dev. 2018;145:1–10. https://doi.org/10.1242/dev.165753
900 49. Choi HMT, Chang JY, Trinh LA, Padilla JE, Fraser SE, Pierce NA. Programmable in situ
901 amplification for multiplexed imaging of mRNA expression. Nat Biotechnol. Nature
902 Publishing Group; 2010;28:1208–12. https://doi.org/10.1038/nbt.1692
903 50. Álvarez JA, Díaz-Benjumea FJ. Origin and specification of type II neuroblasts in the
904 Drosophila embryo. Dev. 2018;145:1–10. https://doi.org/10.1242/dev.158394
905 51. Brunner D, Dücker K, Oellers N, Hafen E, Scholzi H, Klambt C. The ETS domain protein
906 Pointed-P2 is a target of MAP kinase in the Sevenless signal transduction pathway. Nature.
907 1994;370:386–9. https://doi.org/10.1038/370386a0
908 52. Klambt C. The Drosophila gene pointed encodes two ETS-like proteins which are
909 involved in the development of the midline glial cells. Development. 1993;117:163–76.
910 https://doi.org/10.1242/dev.117.1.163
911 53. Bullinger G. Conservation and divergence of the retinal homeobox genetic neural lineage
912 between Drosophila melanogaster and Tribolium castaneum. University of Göttingen; 2024.
913 http://dx.doi.org/10.53846/goediss-10513
914 54. Dreyer D, Vitt H, Dippel S, Goetz B, el Jundi B, Kollmann M, et al. 3D standard brain of
915 the red flour beetle Tribolium castaneum: a tool to study metamorphic development and
916 adult plasticity. Front Syst Neurosci. 2010;4:1–13.
917 http://journal.frontiersin.org/article/10.3389/neuro.06.003.2010/abstract
918 55. Steinmetz PRH, Urbach R, Posnien N, Eriksson J, Kostyuchenko RP, Brena C, et al. Six3
919 demarcates the anterior-most developing brain region in bilaterian animals. Evodevo.
920 BioMed Central Ltd; 2010;1:14. http://www.evodevojournal.com/content/1/1/14
921 56. Posnien N, Koniszewski N, Bucher G. Insect Tc-six4 marks a unit with similarity to
922 vertebrate placodes. Dev Biol. Elsevier Inc.; 2011;350:208–16.
923 http://dx.doi.org/10.1016/j.ydbio.2010.10.024
924 57. Urbach R, Technau GM. Neuroblast formation and patterning during early brain
925 development in Drosophila. BioEssays. 2004;26:739–51. https://doi.org/10.1002/bies.20062
926 58. Bier E, Vaessin H, Younger-shepherd S, Jan LY. deadpan, an essential pan-neural gene in
927 Drosophila ,encodes a helix-loop-helix protein similar to the hairy gene product. Genes Dev.
928 1992;2137–51. 10.1101/gad.6.11.2137
929 59. Li X, Xie Y, Zhu S. Notch maintains Drosophila type II neuroblasts by suppressing
930 expression of the Fez transcription factor Earmuff. Development. 2016;143:2511–21.
931 http://dev.biologists.org/lookup/doi/10.1242/dev.136184
932 60. Campos-Ortega JA, Hartenstein V. The embryonic development of Drosophila
933 melanogaster. 1st ed. Berlin, Heidelberg: Springer; 1985.
934 61. de Velasco B, Erclik T, Shy D, Sclafani J, Lipshitz H, McInnes R, et al. Specification and
935 development of the pars intercerebralis and pars lateralis, neuroendocrine command
936 centers in the Drosophila brain. Dev Biol. 2007;302:309–23.
937 https://doi.org/10.1016/j.ydbio.2006.09.035
938 62. Hwang HJ, Rulifson E. Serial specification of diverse neuroblast identities from a
939 neurogenic placode by Notch and Egfr signaling. Development. 2011;138:2883–93.
940 https://doi.org/10.1242/dev.055681
941 63. Lee HH, Frasch M. Survey of Forkhead Domain Encoding Genes in the Drosophila
942 Genome: Classification and Embryonic Expression Patterns. Dev Dyn. 2004;229:357–66.
943 https://doi.org/10.1002/dvdy.10443
944 64. Schinko JB, Weber M, Viktorinova I, Kiupakis A, Averof M, Klingler M, et al. Functionality
945 of the GAL4/UAS system in Tribolium requires the use of endogenous core promoters. BMC

Dev Biol. 2010;10. https://doi.org/10.1186/1471-213X-10-53
65. Schinko JB, Hillebrand K, Bucher G. Heat shock-Mediated misexpression of genes in the beetle Tribolium castaneum. Dev Genes Evol. 2012;222:287–98. https://doi.org/10.1007/s00427-012-0412-x
66. Berghammer AJ, Klingler M, Wimmer E a. A universal marker for transgenic insects. Nature. 1999;402:370–1. http://www.ncbi.nlm.nih.gov/pubmed/10586872
67. Gratz SJ, Ukken FP, Rubinstein CD, Thiede G, Donohue LK, Cummings AM, et al. Highly specific and efficient CRISPR/Cas9-catalyzed homology-directed repair in Drosophila. Genetics. 2014;196:961–71. https://doi.org/10.1534/genetics.113.160713
68. Buescher M, Oberhofer G, Garcia-Perez NC, Bucher G. A Protocol for Double Fluorescent In Situ Hybridization and Immunohistochemistry for the Study of Embryonic Brain Development in Tribolium castaneum. Methods Brain Dev. 2020. p. 219–32. https://link.springer.com/protocol/10.1007/978-1-4939-9732-9_12
69. Tidswell ORA, Benton MA, Akam M. The neuroblast timer gene nubbin exhibits functional redundancy with gap genes to regulate segment identity in Tribolium. Dev. 2021;148. https://doi.org/10.1242/dev.199719
70. Schindelin J, Arganda-Carreras I, Frise E, Kaynig V, Longair M, Pietzsch T, et al. Fiji: An open source platform for biological image analysis. Nat Methods. 2012;9:676–82. https://doi.org/10.1038/nmeth.2019

Acknowledgements

We would like to thank Claudia Hinners for technical support with molecular biology methods, and Elke Küster for help with screening and beetle stock keeping. We also thank Christoph Viehbahn for valuable feedback on the project. Author Simon Rethemeier was supported by a scholarship of the *Göttingen Promotionskolleg für Medizinstudierende*, funded by the *Jacob-Henle-Programm*.